© 2020. Published by The Company of Biologists Ltd | Journal of Experimental Biology (2020) 223, jeb225987. doi:10.1242/jeb.225987

RESEARCH ARTICLE

Development of a comparative chimpanzee musculoskeletal glenohumeral model: implications for human function

Kathleen F. E. MacLean[1,*] and Clark R. Dickerson[2]

ABSTRACT

Modern human shoulder function is affected by the evolutionary adaptations that have occurred to ensure survival and prosperity of the species. Robust examination of behavioral shoulder performance and injury risk can be holistically improved through an interdisciplinary approach that integrates anthropology and biomechanics. Coordination of these fields can allow different perspectives to contribute to a more complete interpretation of biomechanics of the modern human shoulder. The purpose of this study was to develop a novel biomechanical and comparative chimpanzee glenohumeral model, designed to parallel an existing human glenohumeral model, and compare predicted musculoskeletal outputs between the two models. The chimpanzee glenohumeral model consists of three modules – an external torque module, a musculoskeletal geometric module and an internal muscle force prediction module. Together, these modules use postural kinematics, subject-specific anthropometrics, a novel shoulder rhythm, glenohumeral stability ratios, hand forces, musculoskeletal geometry and an optimization routine to estimate joint reaction forces and moments, subacromial space dimensions, and muscle and tissue forces. Using static postural data of a horizontal bimanual suspension task, predicted muscle forces and subacromial space were compared between chimpanzees and humans. Compared with chimpanzees, the human model predicted a 2 mm narrower subacromial space, deltoid muscle forces that were often double those of chimpanzees and a strong reliance on infraspinatus and teres minor (60–100% maximal force) over other rotator cuff muscles. These results agree with previous work on inter-species differences that inform basic human rotator cuff function and pathology.

KEY WORDS: Comparative biomechanics, Evolutionary biomechanics, Musculoskeletal modeling, Shoulder biomechanics

INTRODUCTION

Studies of evolution and biomechanics typically fall into three categories – comparative, experimental and modeling (Pontzer et al., 2009). For evolutionary science, comparative morphometric assessment persistently emerges as a primary historical method to quantify the physical abilities and locomotion of human relatives and ancestors. This often involves comparisons of single skeletal features, or a series of skeletal features from fossils for association of form with function with extant hominids such as humans and the great apes (Young, 2008). Experimental studies complement morphometric analyses, typically by quantifying and comparing locomotor and evolutionarily relevant tasks between different primate species (Bertram and Chang, 2001; Demes and Carlson, 2009; Larson, 1988; Larson and Stern, 2013; Stern and Larson, 2001). Experimental research quantifies differences between species in locomotor behavior, and provides clues as to probable adaptions following divergence from a common ancestor. However, both methods include problematic aspects. Although bone shape has been linked to function (Oxnard, 1969), the individual plasticity of skeletal features and the effect of external stimuli in altering morphological features reduce the correlation (Collard and Wood, 2000; Young, 2005). Comparative experimental work, while highly valuable, has been limited by subject availability and compliance, and procedural modifications for non-human subjects may reduce data precision and generalizability (Stevens and Carlson, 2008). Computational biomechanical models offer an alternative to morphological and experimental approaches by incorporating properties of musculoskeletal function and motor control dynamics using information obtained from musculoskeletal structure to simulate functionality (Hutchinson, 2012).

The modern human shoulder is primarily adapted for non-locomotor, below shoulder-height behaviors, despite a possible arboreal ancestry (Arias-Martorell, 2019; Larson, 2007; Lewis et al., 2001; Oxnard, 1969; Thorpe et al., 2007; Veeger and van der Helm, 2007; Young et al., 2015). The subacromial space is the area between the humeral head and the acromion of the scapula, through which the supraspinatus tendon passes (Bey et al., 2007). This space is narrow, as a result of a laterally projecting acromion that often slopes inferiorly (Voisin et al., 2014). But as the human arm elevates, the width of the subacromial space decreases further, reducing the space the supraspinatus tendon occupies. This increases the risk for impingement of the supraspinatus tendon and initiation of rotator cuff pathology (Bey et al., 2007; Graichen et al., 2001). The high musculoskeletal demands placed on the human shoulder during overhead tasks also make this a difficult posture to maintain without fatigue and fatigue-related disorders, particularly of the rotator cuff (Dickerson et al., 2015; Ebaugh et al., 2006a,b; Grieve and Dickerson, 2008; Rashedi et al., 2014). The human rotator cuff muscles fatigue rapidly in overhead postures, affecting muscular coordination at the glenohumeral joint and causing scapular and humeral dyskinesis (Chopp et al., 2010; Cote et al., 2009; Teyhen et al., 2008). Overhead postures become even more problematic as workload increases or the posture is sustained for longer periods (Ebaugh et al., 2006b). Humans who engage in climbing for sport or recreation experience an extremely high rate of upper extremity injury (Folkl, 2013; Nelson et al., 2017), with reports of rotator cuff tendonitis and impingement in climbing populations as high as 33% (Rooks, 1997). Conversely, closely related primates, like chimpanzees, regularly assume and maintain high force overhead climbing and suspensory postures

[1]Division of Kinesiology, School of Health and Human Performance, Dalhousie University, 6260 South Street, Halifax, NS, Canada B3H 4R2. [2]Department of Kinesiology, University of Waterloo, Waterloo, ON, Canada N2L 3G1.

*Author for correspondence (kathleen.maclean@dal.ca)

K.F.E.M., 0000-0001-8632-3131; C.R.D., 0000-0003-1550-9777

Received 31 March 2020; Accepted 1 October 2020

Journal of Experimental Biology (2020) 223, jeb225987. doi:10.1242/jeb.225987

without developing shoulder pathology (Potau et al., 2007; Stern and Larson, 2001). Despite humans having a likely arboreal common ancestor with chimpanzees (Kivell and Schmitt, 2009; Lovejoy et al., 2009; Thorpe et al., 2007, 2014), the human shoulder appears to have musculoskeletally devolved a capacity for overhead activities (Ebaugh et al., 2006a; Lewis et al., 2001; Oxnard, 1969; Punnett et al., 2000). To date, there have been few anthropological computational models of the upper extremity (Regnault and Pierce, 2018), and no upper extremity musculoskeletal model analyzing the human evolutionary path and evolutionary holdovers defining modern human musculoskeletal shoulder capacity.

As chimpanzees are the closest genetic living relative to humans, a chimpanzee shoulder model that parallels a human shoulder model (Dickerson et al., 2007) could provide novel insights into the history of human arborealism and its relationship to the form of the present human shoulder. Chimpanzees and humans share a similar shoulder structure and function (Young et al., 2015). Though specific differences exist which help to delineate the two, both chimpanzees and humans have shoulder bone shape and musculature that defines the great ape morphotype as distinct from other primates (Larson, 1998; Swindler and Wood, 1973; Young, 2003, 2008). Resultantly, the two species have a large amount of functional overlap at the shoulder. Chimpanzees possess a hybrid upper extremity that enables both arboreal and terrestrial quadrupedal locomotion, some suspensory brachiation and bipedalism, and non-locomotor behaviors (Cartmill and Smith, 2009). In contrast, humans have an upper extremity that has devolved any locomotor utility in favor of primarily non-locomotor, non-weight bearing, below shoulder height behaviors such as carrying, reaching, tool making and use, and throwing (Cartmill and Smith, 2009; Lewis et al., 2001; Veeger and van der Helm, 2007). While humans can perform locomotor behaviors such as climbing, and may have ancestral ties to them, the modern efficiency, comfort and sustainability is limited (Folkl, 2013; Nelson et al., 2017). As the chimpanzee represents a similar musculoskeletal system to humans that shares general functional shoulder ability, but with a greater ancestral arboreal capacity, it represents a useful comparative model. Comparative human and chimpanzee musculoskeletal shoulder models will aid in determining what morphological features functionally distinguish the species. These models can also provide insights into the evolutionary form and function relationship of the modern human shoulder.

The purpose of this study was to develop a novel model of the chimpanzee shoulder that parallels the human Shoulder Loading and Assessment Modules (SLAM) model created by Dickerson and colleagues (2007). The model was evaluated using electromyographical data on chimpanzees from the Stony Brook Primate Locomotion Laboratory (Larson and Stern, 1986; Larson et al., 1991; S. Larson, Stony Brook University, unpublished data). The muscular and subacromial space width outputs of this model were compared with those from the existing human shoulder model in an attempt to better delineate those musculoskeletal features that inhibit human performance of overhead behaviors. It was hypothesized that the human model would predict higher muscle forces across all muscles as a percentage of maximal force-producing capability determined by muscle cross-sectional area, but particularly in the rotator cuff muscles, as well as a narrower subacromial space, compared with the chimpanzee model predictions. This would be due to humans having a lower muscle mass and PCSA, and a more laterally projecting acromion, respectively.

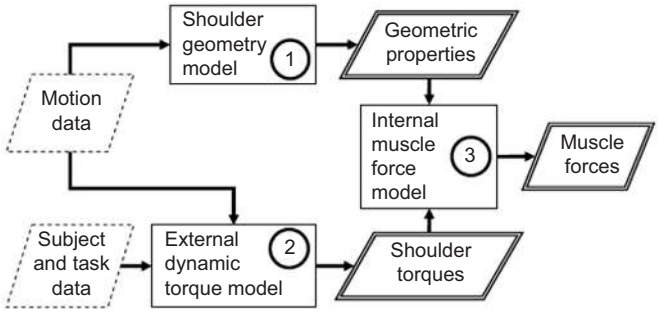

Fig. 1. General template of the inputs, modules and outputs that define the original human SLAM model and novel chimpanzee model. The original SLAM (Shoulder Loading and Assessment Modules) model, created by Dickerson et al. (2007). Inputs are in dashed boxes, modules (1–3) are in black lined boxes and outputs are in double-lined boxes. The overall structure was followed for the chimpanzee model with chimpanzee-specific inputs and module parameters. Most differences between models occurred in the geometric properties module.

MATERIALS AND METHODS

Model structure

The chimpanzee model is designed to perform comparator analyses with parallel models of other species, such as humans. Outputted predictions from the chimpanzee model are not intended to produce standalone musculoskeletal predictions of chimpanzee shoulder function. The model provides insight into the differences in musculoskeletal function that can manifest between two species models in an analogous computational platform based on differences in geometric musculoskeletal form. Geometric musculoskeletal differences that can be examined include muscle moment arms, muscle force predictions, total muscle force, joint forces and moments, and glenohumeral joint stability.

This study required assembly of a novel chimpanzee glenohumeral musculoskeletal model of the right arm, using the template of an extant human SLAM model (Fig. 1) (Dickerson et al., 2007). Like the SLAM model, the chimpanzee glenohumeral model is composed of three inter-connected modules: (1) a musculoskeletal geometry module; (2) an external dynamic moment module; and (3) an internal muscle force prediction module. The primary inputs for these modules include average species anthropometric data, motion data and task-specific data. Motion data are kinematic motion capture marker positions, while task-specific data are the task-specific hand forces. The outputs of the geometry and moment modules produce the necessary inputs for the force prediction module, which uses an optimization routine to solve for muscle forces. Most differences between the two species-specific models were implemented in the geometry module, but all three modules were modified to represent the chimpanzee.

Task-specific input

The task analyzed in this study was a single overhead horizontal bimanual arm suspension cycle. This task was chosen as it is considered to be a common ancestral behavior in the two species, and it is completed with very different levels of capability in modern chimpanzees and humans. Chimpanzees still habitually climb and suspend, while humans appear to no longer have a weight-bearing upper extremity suitable for locomotive purposes (Wood and Richmond, 2000).

The model was used to assess six different instances within the horizontal bimanual arm suspension cycle. (1) Early right support – double support phase. (2) Mid right support – left swing, single support phase. (3) Late right support – double support phase.

Journal of Experimental Biology (2020) 223, jeb225987. doi:10.1242/jeb.225987

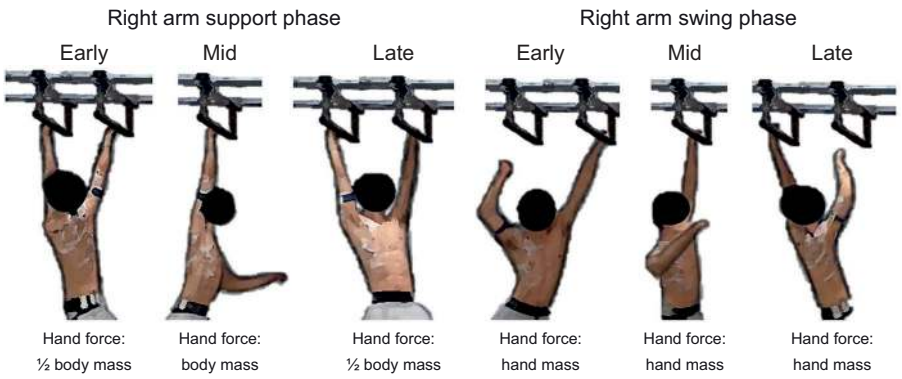

Fig. 2. A visualization of the six static instances of the horizontal bimanual arm suspension cycle. The suspension cycle has two phases: a right arm support phase, during which the right arm maintains contact with the support bar, and a right arm swing phase, during which the right arm swings forward toward the next sequential bar. Each phase is broken down into three additional instances: early, mid and late support or swing. The hand force for each phase was assumed based on which hands were in contact with the support bars.

(4) Early right swing – down phase of arm swing. (5) Mid swing – beginning of reach phase of arm swing. (6) Late swing – pre-contact with support rung.

These six instances represent distinct time points of the suspension cycle that require different levels of muscular support to move and stabilize the body and upper extremity (Larson and Stern, 1986; Larson et al., 1991). These six instances, along with the task-specific hand forces applied at each instance, can be seen in Fig. 2.

Musculoskeletal geometry module

The original SLAM geometry module uses human representative bone scan data and postural motion coordinate data as inputs to determine boney orientations and positions of each segment, and subsequent lines of action and moment arms for each muscle element (Dickerson et al., 2007). The chimpanzee module paralleled this structure. When original chimpanzee musculoskeletal data were available, they were used in the geometric module. If original quantitative chimpanzee data were not available, musculoskeletal geometry was mathematically and iteratively fitted to the model to provide an appropriate representation of chimpanzee musculoskeletal geometry, as has been done in previous models (O'Neill et al., 2013). There are five different parts of the musculoskeletal geometry module.

The first part of the geometric module is a segment parameter definition. The model has five segments – the torso, and the right-side clavicle, scapula, humerus and forearm. The glenohumeral joint is modeled as a spherical joint with three degrees of rotational freedom. As the utility of the model is for shoulder and glenohumeral analysis, the forearm is visually modeled as a simplified, single radial/ulnar link with the elbow having one degree of freedom (flexion/extension) (Fig. 3). Pronation and supination of the forearm were still accounted for in the model in the external moment module (see 'External dynamic moment module', below) to calculate the three-dimensional elbow angles, forces and moments, which were used to drive the final internal force prediction module. The dimensions of each of the segments for the constructed chimpanzee model were determined from existing data on average bone dimensions in the chimpanzee upper extremity (Larson, 1998; Schoonaert et al., 2007; Thorpe et al., 1999; Young, 2003).

The second part of the geometric module is an algorithm for shoulder rhythm. Shoulder rhythm is the closed-chain kinematic interaction between the bones and joints of the shoulder (Inman et al., 1944). Measuring this kinematic interaction can be difficult, as movement of the scapula and clavicle is particularly hard to acquire with skin surface marker motion capture methods, the most commonly used approach for quantifying three-dimensional kinematics (Karduna et al., 2001; van Andel et al., 2009). Assessment of shoulder rhythm is also difficult because of individual variation. Measured shoulder rhythm has been shown to be highly variable across individuals and populations (Grewal and Dickerson, 2013; Grewal et al., 2017; Ludewig and Cook, 2000; Ludewig et al., 2009; McClure et al., 2001; Tsai et al., 2003). However, several invasive studies have demonstrated a predictable kinematic pattern in scapular and clavicular three-dimensional motion with respect to the more easily acquired humeral and thoracic motion (Högfors et al., 1991; Karduna et al., 2001; van Andel et al., 2009). Therefore, mathematical equations are used to predict three-dimensional scapular and clavicular rotations from the measured three-dimensional kinematics of thoracohumeral rotations. Mathematically predicted shoulder rhythm is characterized by a total of six equations representing three clavicular rotations and three scapular rotations. Each shoulder rhythm equation contains mean value coefficients for the population and they do not change between individuals. Thus, two individuals with the same three-dimensional thoracohumeral orientation will have the same equation-predicted scapular and clavicular three-dimensional orientations, though individual variation may result in different true scapular and clavicular orientations. A number of human shoulder rhythm equations have been published to estimate clavicular and scapular kinematics from thoracohumeral skin surface motion capture. Those produced by Grewal and Dickerson

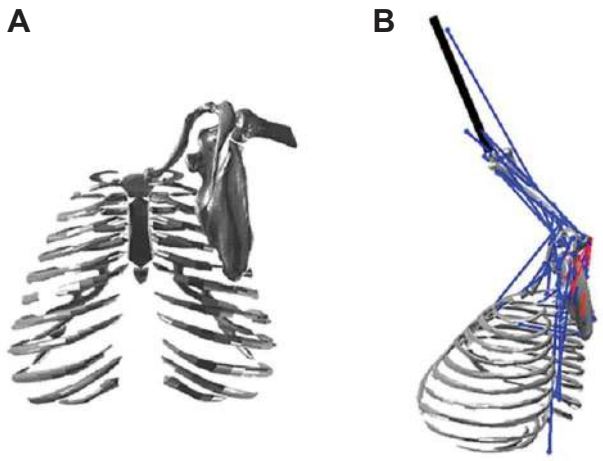

Fig. 3. Visualization of the chimpanzee glenohumeral model developed in custom-written Matlab software. (A) The orientation of the humerus, scapula, clavicle, sternum and torso bone segments. The forearm was modeled as a rigid link. (B) Muscles were modeled as strings, and three-dimensional origins and insertions were identified within each applicable bone's three-dimensional space. Where appropriate, muscle paths were wrapped around bones using cylindrical and spherical wrapping techniques.

(2013) were used in the human model, as they account for a large range of humeral elevation, much like that assumed during bimanual horizontal climbing (Grewal and Dickerson, 2013). No shoulder rhythm equations currently exist for chimpanzees.

The mathematical representation of the chimpanzee shoulder rhythm (Eqns 1–6) was developed by estimating and simulating modified scapular and clavicular orientations of the chimpanzee shoulder from previously developed human shoulder rhythm equations (Grewal and Dickerson, 2013). Briefly, the three-dimensional orientation of the clavicle and scapula were initially estimated using human shoulder rhythm equations (Grewal and Dickerson, 2013). Rotational and translational modifications of clavicular and scapular position were then manually and iteratively made in static arm postures to re-orient both segments to an appropriate chimpanzee orientation, aided by x-rays of the chimpanzee shoulder girdle (Thompson et al., 2020). In the x-rays, a chimpanzee was prone on a table, with the arm to the side, abducted between 0 and 90 deg. Once a satisfactory position and orientation were achieved, three-dimensional anatomical landmarks on the torso, humerus, clavicle and scapula were recorded in the static posture. This process was repeated in a series of static postures ranging in degree of thoracohumeral elevation. From the compiled three-dimensional landmark data, three-dimensional bone rotations were calculated following International Society of Biomechanics (ISB) standards (Wu et al., 2005) and used to develop novel predictive chimpanzee shoulder rhythm equations (Eqns 1–6). The r^2 values for these equations fell between 0.42 and 0.75, a range that has been reported in human shoulder rhythm derivations previously (Xu et al., 2014). These equations were incorporated into the model to define the orientation of the scapula and clavicle with respect to the humerus and torso:

$$\gamma_{S,chimp} = -3.91 + (0.354)(\gamma_{TH0}) + (-0.232)(\beta_{TH}) + (-0.0029)(\gamma_{TH0})(\beta_{TH}), \quad (1)$$

$$\beta_{S,chimp} = 20.28 + (0.0806)(\gamma_{TH0}) + (0.2087)(\beta_{TH}) + (0.0042)(\gamma_{TH1}) + (0.00103)(\gamma_{TH0})(\gamma_{TH1}), \quad (2)$$

$$\alpha_{S,chimp} = 28.18 + (-0.0062)(\gamma_{TH0}) + (0.1017)(\beta_{TH}) + (0.029)(\gamma_{TH1}), \quad (3)$$

$$\gamma_{C,chimp} = -4.2 + (0.283)(\gamma_{TH0}) + (0.145)(\beta_{TH}) + (0.1992)(\gamma_{TH1}), \quad (4)$$

$$\beta_{C,chimp} = -40.52 + (0.249)(\beta_{TH}) + (0.011)(\beta_{TH}^2) + (-0.1108)(\gamma_{TH1}), \quad (5)$$

$$\alpha_{C,chimp} = 67.0 + (0.136)(\gamma_{TH0}) + (0.245)(\beta_{TH}) + (0.1049)(\gamma_{TH1}) + (0.00109)(\beta_{TH})(\gamma_{TH1}). \quad (6)$$

Eqns 1–6 predict the chimpanzee scapular retraction/protraction (γ_S), scapular lateral/medial rotation (β_S), scapular anterior/posterior tilt (α_S), clavicular elevation/depression (γ_C), clavicular retraction/protraction (β_C), and clavicular forward/backward rotation (α_C). The three thoracohumeral rotations used to predict the scapular and clavicular rotations are represented as plane of elevation (γ_{TH0}), elevation (β_{TH}), and internal/external rotation (γ_{TH1}).

The third and fourth parts of the geometry module are the definition of right-side muscle elements and their corresponding lines of action (Fig. 3). Fourteen separate upper extremity muscles were modeled. In both the chimpanzee and human geometry module, five of these muscles – biceps, triceps, infraspinatus, supraspinatus and deltoids – were modeled with multiple mechanical elements to represent their multiple attachments for a total of 20 muscle elements. Chimpanzees share most of the same muscular anatomy with humans. The exception is that chimpanzees have an additional muscle, the dorsoepitrochlearis (Ashton and Oxnard, 1963; Diogo et al., 2013; Swindler and Wood, 1973). The dorsoepitrochlearis muscle typically arises from the latissimus dorsi or coracoid process and attaches on the distal humerus (Ashton and Oxnard, 1963). Muscle attachment sites were determined using published data (Ashton and Oxnard, 1963; Ashton et al., 1976; Carlson, 2006; Diogo et al., 2013; Swindler and Wood, 1973; Thorpe et al., 1999). Precise three-dimensional locations were not available for chimpanzee muscle origins and insertions. Estimations were made iteratively following muscle footprints provided in literature sources (Swindler and Wood, 1973). Muscle lines of action were defined as strings, partially using spherical and cylindrical geometric muscle wrapping techniques around orthopedic surfaces that generate more physiologically representative lines of action and paths about the glenohumeral joint in chimpanzees (Fig. 3) (Dickerson et al., 2007; van der Helm, 1994). While modeling muscles as strings is an oversimplification of muscle physiology and architecture, 'overfitted' muscle models can result in erroneous muscle force predictions and generally have limited predictive capabilities (Buchanan et al., 2004; Scott and Winter, 1991). The fifth and final part of the module created contact force application sites between the scapula and ribcage, as well as ligament placements. Ligaments were not included as contributing elements in either model.

The postural motion data inputs for the chimpanzee model geometric module were derived from human motion capture files. Quantitative three-dimensional data, sufficient as inputs to the geometry module, do not currently exist of chimpanzees performing brachiation tasks, including horizontal bimanual arm suspension (Demes and Carlson, 2009; Reghem et al., 2013; Stern and Larson, 2001; Usherwood et al., 2003). In the absence of three-dimensional chimpanzee kinematics, human arm suspension kinematics were systematically modified to anthropometrically represent chimpanzee segment lengths and joint positions (MacLean and Dickerson, 2019). Appropriate chimpanzee arm lengths were achieved by translating the wrist and elbow joint centers, each of which were defined by human skin surface marker positions, to modify the forearm and upper arm length, respectively, to those reported in the literature (Schoonaert et al., 2007). As chimpanzees also have a more superiorly and medially positioned scapula, it was also necessary to shift the human acromion marker both superiorly and medially by a standardized distance based on the chimpanzee x-rays (Thompson et al., 2020). As the glenohumeral joint position is estimated from the position of the acromion marker, this automatically shifted the chimpanzee glenohumeral joint. Once joint centers were translated, these data were used as a surrogate for chimpanzee arm suspension kinematics. For the purpose of this analysis, the kinematic data of a single experienced climber were used for the simulation. Outputs of an average single subject delineate mean differences between species, and provide an initial indication of the realism of the comparative models that could be washed out through population means. Multi-subject analyses can be performed within each model, with appropriate subject kinematic, anthropometric and task data to further explore the influence of performance variation.

External dynamic moment module

The external dynamic moment module uses motion capture data to derive external forces and moments using inverse dynamics

Journal of Experimental Biology (2020) 223, jeb225987. doi:10.1242/jeb.225987

(Dickerson et al., 2007). The moment module was driven by the same modified human motion capture data inputs used to drive the geometric module. An inverse dynamics approach was used to calculate joint forces and moments (Vaughan et al., 1992).

The moment module has four steps. The first was the description of segment properties. Segment properties of the chimpanzee upper extremity (upper arm, forearm and hand) were determined using anthropometric data on segment mass, length and moments of inertia (Thorpe et al., 1999; Schoonaert et al., 2007; Zihlman, 1992). The modified human motion data were used to estimate the center of rotation for the glenohumeral, elbow and wrist joints, which were also used to determine locations of the segmental centers of mass (Dickerson et al., 2007). Local coordinate systems for each segment were then defined.

The second and third parts of the module are the calculation of linear and angular kinematics. These were determined from differentiating filtered motion data and the Euler angle decomposition method employed by Dickerson et al. (2007). For the purposes of the current static analysis, this step was not utilized. However, it is present in the module for the possibility of dynamic analyses.

The fourth step is the calculation of external joint forces and net moments. Forces and moments were calculated using Newtonian laws of motion (Vaughan et al., 1992). Gravity was the only external force applied, with the reaction force acting at the hand. In the swing phase of the suspension cycle, this translated to an external force equivalent to the gravitational force produced by the masses of the upper body segments. In the mid-support phase of the suspension cycle, when only the right hand provided support, the external force acting at the hand was assumed to be equivalent to total body mass multiplied by gravity. At early and late support, the external force was assumed to be equally shared by the two limbs and was half of body mass multiplied by gravity, and applied at the right hand.

Internal muscle force prediction module

The outputs of both the geometry and moment modules provide inputs to the muscle force prediction module (Fig. 1). The high number of muscles that contribute to glenohumeral motion constitute an indeterminate system, with more muscles than mechanical equations to define the system (Dickerson et al., 2007). Thus, an optimization approach was used to generate muscle force predictions using muscular and mechanical constraints. The optimization routine consists of five interconnected parts that delimit potential force prediction solutions, enhancing physiological feasibility.

First, a series of mechanical constraints were defined for the three-dimensional angular and linear equilibrium of the glenohumeral joint, composed of muscle forces, joint contact forces and external forces. An additional mechanical constraint was enforced for elbow joint flexion/extension moment equilibrium.

Second, muscle force bounds were defined. The lower bound for all muscles was 0, while the upper bound was proportional to the absolute physiological cross-sectional area (PCSA) of each chimpanzee muscle, based on published data (Table 1) (Carlson, 2006; Kikuchi, 2010; Michilsens et al., 2009; Mathewson et al., 2014; Oishi et al., 2009; Thorpe et al., 1999; Ward et al., 2006), multiplied by a specific tension value. As no data exist for baseline muscle tension in chimpanzees, the previously used specific tension for humans of 88 N cm^{-2} was applied to determine muscle force upper bounds (Wood et al., 1989). Chimpanzee subscapularis and infraspinatus PCSA data were only provided as whole muscle, and not the three and two respective mechanical elements of each muscle. To determine appropriate mechanical muscle element PCSAs for subscapularis and infraspinatus, the percentage breakdown of PCSA for the elements of these muscles in humans was used to assume a PCSA of the mechanical muscle elements for chimpanzees.

Third, another constraint, glenohumeral contact force, was applied. Derived glenohumeral stability force ratios were implemented to determine force thresholds in eight directions perpendicular to the surface of the glenoid (Lippitt et al., 1993). As glenohumeral stability force ratios were unknown in chimpanzees, they were estimated through known structural differences between species in glenoid shape and depth (Larson, 1998; Lippitt et al., 1993; Macias and Churchill, 2015; Matsen et al., 1994; Young, 2003). The human glenoid fossa is approximately 4.8 mm deep, inclusive of the labrum, whereas the chimpanzee fossa was determined to be approximately 6 mm deep. According to Matsen and colleagues (1994), stability ratios increase 10.9% for every 1 mm increase in depth. As the chimpanzee glenoid fossa is of a similar shape to that of humans, it was assumed to have a proportionally similar increase of 13.13% in stability force ratios in all eight directions as a result of increased depth.

Fourth, the objective function of the optimization routine was defined (Eqn 7):

$$\Theta = \sum_{i=1}^{20} \left(\frac{f_i}{\mathrm{PCSA}_i} \right)^3, \quad (7)$$

where the objective function, Θ, represents the summation of the individual cubes of the muscle stresses, and f_i and PCSA_i represent the

Table 1. Muscle PCSA for all elements included in the force prediction module of the human and chimpanzee glenohumeral model

	Absolute PCSA (cm^2)		Relative PCSA (cm^2 kg^{-1})	
Muscle	Human	Chimpanzee	Human	Chimpanzee
Dorsoepitrochlearis	n/a	2.98	n/a	0.066
Deltoid middle	7.42	28.95	0.103	0.643
Deltoid posterior	4.29	11.06	0.060	0.246
Deltoid anterior	8.84	12.10	0.123	0.269
Coracobrachialis	1.58	7.85	0.022	0.174
Infraspinatus 1 (upper)	6.37	11.08	0.088	0.246
Infraspinatus 2 (lower)	7.67	13.34	0.107	0.296
Subscapularis 1 (upper)	2.83	11.19	0.039	0.249
Subscapularis 2 (middle)	3.72	14.71	0.052	0.327
Subscapularis 3 (lower)	5.10	20.17	0.071	0.448
Supraspinatus	3.15	19.92	0.044	0.443
Teres major	8.48	12.69	0.118	0.282
Teres minor	2.81	5.48	0.039	0.122
Biceps (long)	4.94	10.10	0.069	0.224
Biceps (short)	2.18	8.06	0.030	0.179
Triceps (long head)	9.98	15.39	0.139	0.342
Triceps (medial head)	8.98	24.49	0.125	0.544
Triceps (lateral head)	8.98	17.09	0.125	0.380
Brachialis	9.98	20.43	0.139	0.454
Brachioradialis	2.00	8.52	0.028	0.189

Physiological cross-sectional area (PCSA) values are both absolute and relative to the total body mass of the human and chimpanzee individuals used in each model. Human PCSA was acquired from Makhsous (1999). The human data were measured from elderly individuals. As PCSA decreases with age, the values presented here have been doubled to more accurately represent the PCSA of younger, healthy human adults (Dickerson et al., 2007). Chimpanzee PCSA were acquired or derived from Carlson (2006), Kikuchi (2010), Michilsens et al. (2009), Oishi et al. (2009) and Thorpe et al. (1999). Chimpanzee subscapularis and infraspinatus were provided as whole-muscle PCSA, not partitioned. Therefore, the total PCSA values for each of these muscles were partitioned into their elements based on known human percentages of total infraspinatus and subscapularis.

force prediction and physiological cross-sectional area for muscle *i*. This function weighs the muscle force prediction by the absolute PCSA of that muscle and seeks to minimize the summation of the individual cubes of the muscle stresses. It has been used in similar shoulder models and creates force sharing amongst agonistic muscles (Chaffin, 1997; Dickerson et al., 2007; Dul et al., 1984). The model solved for muscle forces, joint contact forces and torques, and directional dislocation force ratio coefficients (Dickerson et al., 2007).

Fifth, the solution methodology was defined. The optimization routine has a standardized scheme made up of the previous parts of the prediction module. The methodology solves for the indeterminacy of the mechanical system in a sequential manner. Each solution is used to inform the next sequential solution.

Chimpanzee shoulder model evaluation

The chimpanzee glenohumeral model was evaluated using a concordance analysis to compare computational model chimpanzee muscle force predictions with experimentally collected chimpanzee electromyographical (EMG) data for a subset of muscles included in the model. Evaluation of the chimpanzee model presented challenges unfamiliar to human modeling efforts. As novel experimental data on chimpanzees cannot be readily acquired because of new legislation and the lack of experimental facilities, model evaluation was limited to comparisons with previously collected EMG data on chimpanzee muscle activity. The tissue loading predicted by the chimpanzee model was assessed through comparison with published and unpublished experimentally acquired EMG data (Larson, 1988; Larson et al., 1991; Larson and Stern, 1992, 2013) using concordance analysis (Dickerson et al., 2008). This analysis determines timing concordance in muscle activity and inactivity between EMG and predicted model muscle forces. If both the EMG and predicted muscle forces predict muscle activity above defined thresholds, there is concordance. If one indicates activity and the other does not, there is discordance (Dickerson et al., 2008). A concordance analysis is appropriate in this scenario, as instantaneous relative EMG amplitudes are highly variable with postures and movements, and normalization methods, and typically show weak relationships with predicted muscle forces (Makhsous, 1999; van der Helm, 1994). As little data exist that include EMG of chimpanzees brachiating, this method also prevents biased evaluation of the predicted muscle forces via a limited EMG dataset. The concordance analysis was used to assess each of the six simulated instances of the suspension cycle, representing six static points of a full horizontal bimanual arm suspension cycle of the right arm.

Studies that have analyzed muscle activity in primates have not conducted maximal voluntary contractions to normalize EMG produced during activity, as it is not logistically possible. EMG from primates is often normalized to the maximal EMG signal produced during the task of interest (Larson et al., 1991; Usherwood et al., 2003). To determine the 'active' or 'inactive' state of a muscle, a predicted model muscle force was considered 'active' if it was greater than 5% of its maximal force producing capacity (Dickerson et al., 2008). Because of possible noise and spurious predictions, chimpanzee EMG signal was considered 'active' if it was above approximately 5% of the maximal produced signal. Only select muscles were included in the concordance analysis, owing to availability of experimental data. These included published data on anterior deltoid, middle deltoid, posterior deltoid, supraspinatus, infraspinatus, subscapularis, teres minor, triceps brachii, teres major and coracobrachialis (Larson, 1988; Larson et al., 1991; Larson and Stern, 1992, 2013). Unpublished data were also retrieved from University of Stony Brook, New York, USA, courtesy of the Department of Anatomy and used in the concordance analysis. These muscles included triceps brachii, coracobrachialis and middle deltoid. Muscles that were modeled as multiple muscle elements were combined for the concordance analysis, as they were experimentally analyzed as a single muscle element.

Data analysis

Once the chimpanzee glenohumeral model development was complete, the novel model was run for evaluation analysis and for comparative analysis with the human SLAM model. Anthropometric, hand force and kinematic postural inputs for both models were applied for model operation, and selected muscle force and subacromial space width outputs were compared between species.

Subject anthropometric and hand force inputs

Anthropometrics were used to approximate segment parameters for determining joint forces and moments in the external dynamic torque module. Representative average healthy human (mass: 72 kg; height: 1.8 m) and chimpanzee (mass: 45 kg; height: 1.32 m) males were used as the criteria subjects within each species-specific glenohumeral model.

Applied hand forces depended on the suspension phase, and were used in the external dynamic torque module to predict joint forces and moments. As the model was run statically, gravity was assumed to be the only external force, and acting at the hand.

Postural input data

The motion data of a single experienced male climber were used as the static postural input for both the human and chimpanzee glenohumeral models. This motion data were modified to be more representative of the chimpanzee shoulder structure for the chimpanzee model.

The two models used the same human kinematic inputs, but with systematic joint position and segment length modifications in the chimpanzee model. Joint orientation was not altered. Therefore, the chimp model and the SLAM model used the same overall static upper body postures as inputs (Fig. 4). The arm is most horizontally adducted and extended forward in late swing and early support. In late support, the arm is horizontally abducted and most elevated, and resultantly also positioned closest to the torso. Arm elevation decreases with the beginning of swing phase as the hand is released from the support rung and begins to horizontally adduct (Fig. 2).

Between-species comparison

Chimpanzee model outputs from the suspension task were compared with those produced by the human SLAM model while conducting the same functional task of horizontal bimanual arm suspension. The comparison between species was made for the six instances of a single right arm suspension cycle. The human SLAM was executed using experimentally measured bimanual suspension kinematics (MacLean and Dickerson, 2019), subject anthropometrics and estimated external hand forces to determine resultant human glenohumeral muscle forces and subacromial space. The chimpanzee model was subsequently executed using the geometrically modified human kinematics to determine subsequent chimpanzee glenohumeral muscle force and subacromial space.

Output-dependent variables compared between human and chimpanzee models included individual muscle force, average normalized muscle force and subacromial space. Individual muscle forces compared between humans and chimpanzees included the rotator cuff (supraspinatus, infraspinatus, subscapularis, teres minor), anterior deltoid, middle deltoid, posterior deltoid, teres

Journal of Experimental Biology (2020) 223, jeb225987. doi:10.1242/jeb.225987

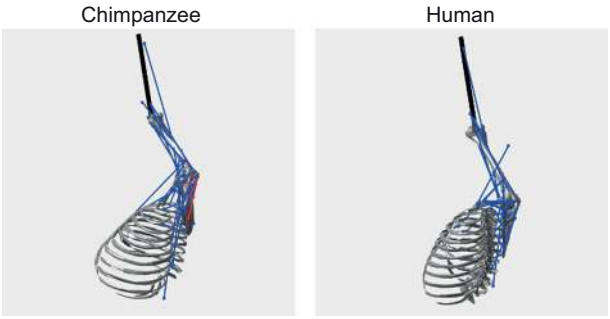

Fig. 4. Posture for both the chimpanzee (left) and human (right) models in the first static instance of the suspension cycle, the early support phase. The same kinematic postural inputs were used in the two models, with manual anthropometric modifications made in the chimpanzee model to correct for joint position and segment lengths.

major, biceps brachii, triceps brachii, coracobrachialis, brachialis and brachioradialis. Each individual muscle's maximal muscle force was determined by dividing the muscle force prediction in Newtons by each muscle's PCSA and specific tension. Muscle forces were normalized to a maximal muscle force, and presented as a percentage of the maximal muscle force, for each muscle for both the human and chimpanzee model. As it is only extant in chimpanzees, analysis of the dorsoepitrochlearis muscle extended only to examination of muscle force sharing predictions in the chimpanzee model. An average normalized muscle force was also reported. All 19 or 20 normalized muscle forces from the human and chimpanzee model, respectively, were also summed and divided by the total number of muscle elements observed in each phasic instance of the suspension cycle to give an indication of the average normalized requirement from the glenohumeral musculature as a percentage, for each species. Subacromial space was the distance between the inferior portion of the acromion and the most superior point of the humeral head.

For this initial analysis, each model simulation was run once to produce single values for each of the dependent variables for an average human and chimpanzee. This precluded the use of typical statistical analyses for determining significant differences between species in shoulder biomechanics. Differences between species are thus presented as an observation of differences between average chimpanzees and humans in shoulder function and physical capability.

RESULTS

Chimpanzee model evaluation

To evaluate the chimpanzee glenohumeral model, muscle force predictions were compared with chimpanzee experimental electromyographical muscle activations while performing the same task – horizontal bimanual arm suspension across all six cycle instances. When both model and experimental data showed activity, concordance was indicated. A total of 12 muscles at 6 discrete time points were used to determine concordance between predicted and observed muscle activity, for a total of 72 data points. Concordance occurred – both model and EMG predicting on or off – in 46 of 72 data points, or 63.8%.

Comparative model outputs

Predicted muscle forces were very different between species. The human infraspinatus lower muscle element was recruited to maximal force and the teres minor to nearly maximal force in early support (Fig. 5A,D). The human model predicted no supraspinatus and a very low late support phase subscapularis contribution in humans (Fig. 5B,C). Chimpanzees were predicted to have more evenly dispersed rotator cuff forces. Humans were predicted to have greater muscle force contributions from all portions of the deltoid than chimpanzees in the support phase (Fig. 5E). The anterior deltoid was predicted to not contribute to the suspension task in either support or swing phase in the chimpanzee model. The teres major, coracobrachialis and dorsoepitrochlearis were limited contributors to completing the suspension task. Only in the human simulation was the coracobrachialis predicted to contribute to the glenohumeral joint equilibrium in early swing and minimally in late swing (Fig. 5K). The triceps long head and lateral heads were active in chimpanzees during mid-support (Fig. 5H), whereas the triceps long head was a large contributor to the glenohumeral and elbow joint force for support phase in the human model (Fig. 5H). The biceps were more active in the human model, contributing a very high percentage of maximal force in early and mid-swing (Fig. 5G). At the elbow, along with the biceps, humans were predicted to rely mostly on the brachioradialis, with muscle force contributions as high as 70% of maximum force production capability (Fig. 5I). Chimpanzees utilized the brachialis more than humans in mid-support.

Average normalized muscle force was much higher in the human model than in the chimpanzee model during the support phase (Table 2). This difference is less magnified when muscle forces were normalized to body mass, but still continued in early and mid-swing (Table 2). Average normalized muscle force was predicted to be more than 3 times as great in humans in early support. The average normalized force in the swing phase was small for both species.

Chimpanzees had a considerably wider subacromial space than humans in all six phasic instances of the suspension cycle (Fig. 6). Differences between the two species were approximately 2 mm. The chimpanzee subacromial space was narrowest in late support when the arm was the most elevated.

DISCUSSION

This study developed a novel chimpanzee glenohumeral joint model for use in comparative musculoskeletal analyses. Comparisons with a parallel human glenohumeral joint model contrasted the influence of muscular and geometric differences between the humans and chimpanzees. The human glenohumeral model predicted higher muscle forces as a percentage of maximum force-producing capability for most muscles and a narrower subacromial space, mostly supporting the research hypotheses. These directional differences indicate musculoskeletal divergence that may associate functional differences with the evolutionary foundation of modern human rotator cuff function and pathology.

Model evaluation and utility

Evaluation of the novel chimpanzee glenohumeral model through concordance analysis provided evidence of the usefulness of the model. The results of the heuristic concordance analysis demonstrated an agreement between the timing of chimpanzee model predictions of muscle activity and experimental electromyographical measures of muscle activity for the same horizontal bimanual arm suspension task. With moderate agreement between measured and predicted muscle activity, the model can be considered sufficiently biologically realistic (Dickerson, 2005). This step provided the necessary evidence to allow plausible comparative analyses between models.

The concordance analysis did not have complete agreement between model predicted and measured muscle activity timing but

Journal of Experimental Biology (2020) 223, jeb225987. doi:10.1242/jeb.225987

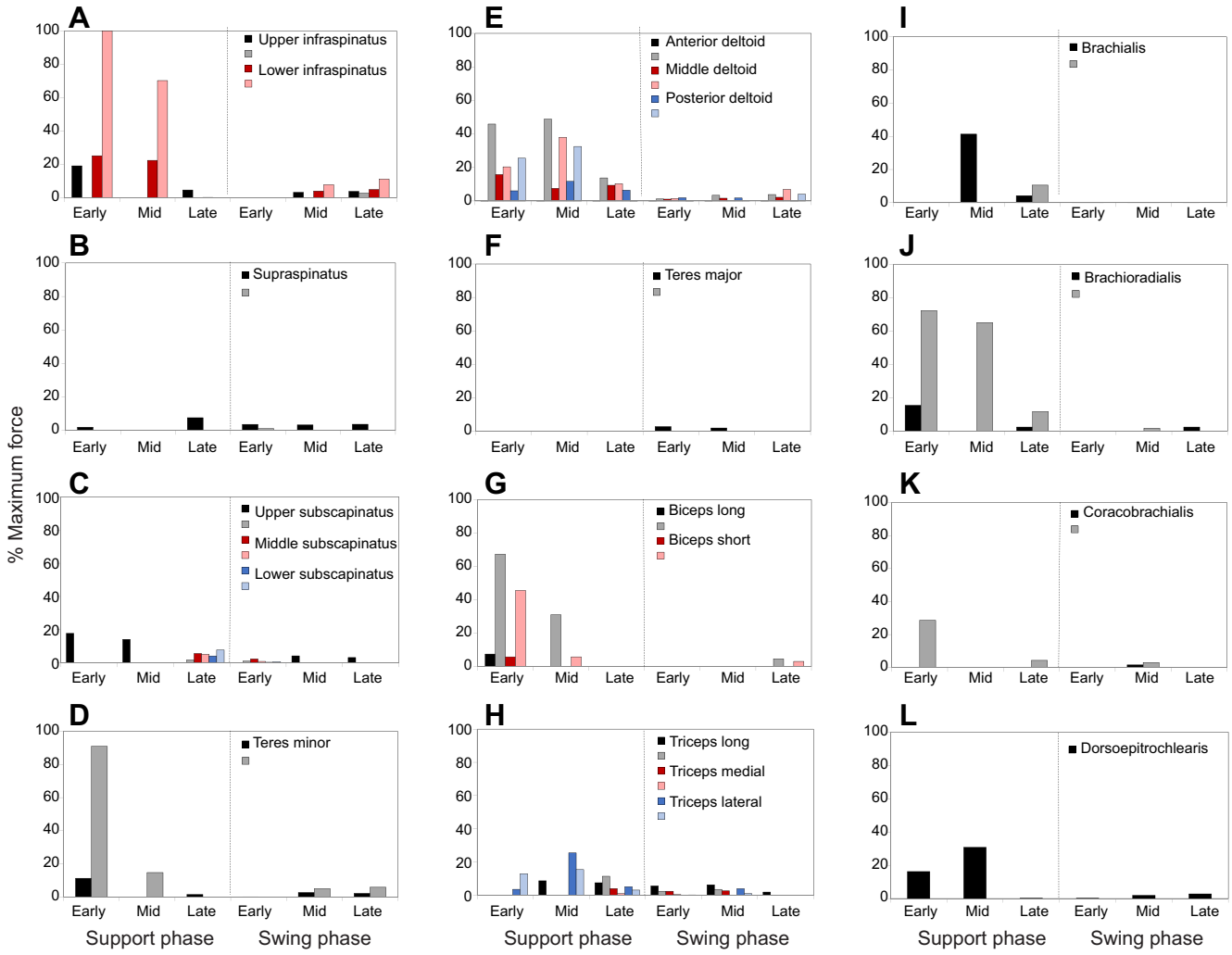

Fig. 5. Predicted chimpanzee and human glenohumeral musculature recruitment, as a percentage of maximum force-producing capability, for six instances of a single right arm suspension cycle. (A) Infraspinatus, (B) supraspinatus, (C) subscapinatus, (D) teres minor, (E) deltoid, (F) teres major, (G) biceps, (H) triceps, (I) brachialis, (J) brachioradialis, (K) coracobrachialis and (L) dorsoepitrochlearis. The right arm suspension cycle includes both a support phase and swing phase, each broken down into three static instances – early, mid and late phase. Early and late support are double support instances, whereas mid-support is during left arm swing and is a single support instance. Chimpanzee muscle force predictions are represented by dark-colored bars of black, red and blue, while human muscle force predictions are in corresponding light-colored bars of grey, red and blue.

Table 2. Chimpanzee and human average total muscle force as a percentage of maximum force and normalized to body mass for each of the six static instances of the right arm suspension cycle

	Average normalized total muscle force (% maximum force)		Average total muscle force normalized to body mass (N kg^{-1})	
Phase instance	Chimpanzee	Human	Chimpanzee	Human
Early support	7.235	26.814	37.22	59.31
Left swing	8.115	16.924	37.44	45.64
Late support	3.159	4.265	22.71	13.42
Early swing	1.027	0.534	6.931	1.647
Mid swing	1.970	1.369	11.54	3.907
Late swing	1.371	2.225	7.606	6.158

Average normalized total muscle force represents all muscle forces as a percentage of their maximum force. Total muscle force normalized to body mass represents all muscle forces normalized to body mass. Average muscle forces were an average of all 20 (chimpanzee) or 19 (human) muscle element's predicted muscle forces, and represent the average predicted muscle force across all muscle elements in a given suspension cycle instance.

the concordance value obtained was moderate. EMG is a very sensitive measurement technique (Basmajian and De Luca, 1985; De Luca, 1997). Thus, the present concordance analysis concentrated on muscle activity timing, as concordance analyses that include muscle amplitudes would be susceptible to EMG variability and Type II error (De Luca, 1997; Miller, 2006). A concordance value of 0.638 is considered satisfactory for an analysis of biological modeling (Dickerson, 2005). Realism in biological modeling is difficult as it requires the consideration of a variety of biological variables dependent on numerous parameters (Dickerson, 2005; Garner and Pandy, 2001).

Differences between the two models mostly represent biological differences in the modeled musculoskeletal systems of the geometric module. The lack of complete biological realism in the chimpanzee model – including some synergistic and antagonistic muscle action – falls within the range of similar biomechanical models (Cholewicki et al., 1995; Dickerson, 2005). The chimpanzee glenohumeral model developed in the present study was and is intended only for muscular

Journal of Experimental Biology (2020) 223, jeb225987. doi:10.1242/jeb.225987

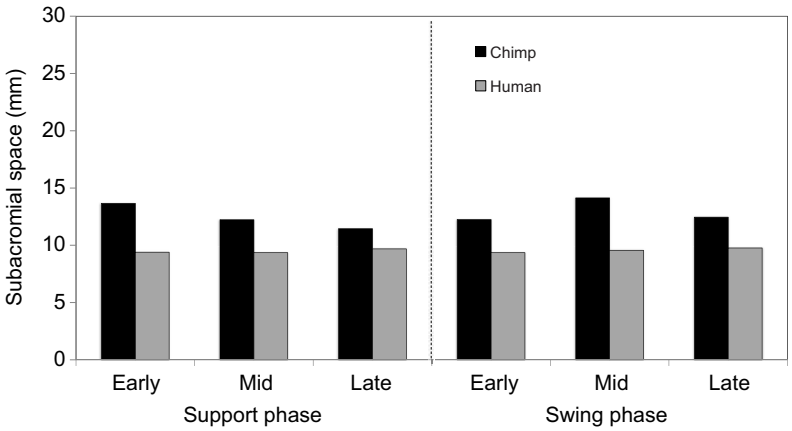

Fig. 6. Predicted chimpanzee and human subacromial space width during a single right arm suspension cycle.

comparison with a parallel representation of the extant human, and future evolutionary models. The model's ability to distinguish different musculoskeletal strategies – particularly muscle force sharing strategies – from other models is its primary objective. As mathematical computational representations of biology, both the human and chimpanzee models represent a simplification of the musculoskeletal system, including a shoulder rhythm to predict scapular and clavicular orientations, muscles modeled as strings, no ligamentous contribution, and an optimization routine for predicting muscle forces. Assumptions and limitations present in the chimpanzee glenohumeral model are structurally mirrored in the comparator model.

The results of the present evaluation demonstrate that the chimpanzee model has value as a comparative model, providing insight into shoulder function and evolution. Compromises and assumptions were essential to develop efficient, purposeful models, but predictions should be viewed in their context. The design of the model limits the generalizability of the present results beyond the above-stated usage and assumptions. However, for performing comparative analyses, these models reflect and highlight real musculoskeletal differences between each species in modeled geometry.

Between-species muscle force predictions

Chimpanzees were predicted to execute the suspension task using an overall lower percentage of their muscular capacity than humans at all discrete stages of the suspension cycle, at both the elbow and glenohumeral joint. This was expected, as chimpanzees have a greater proportional muscle mass in their upper extremity (Walker, 2009). Humans and chimpanzees have approximately 9% and 16% of their total body mass relegated to their upper extremity, respectively (Zihlman, 1992). Despite having a lower average body mass by as much as 25 kg, the chimpanzee upper extremity muscle masses can be upward of twice that of analogous human muscles (Carlson, 2006; Mathewson et al., 2014; Thorpe et al., 1999; Walker, 2009). This translates into individual chimpanzee upper extremity muscles requiring a smaller percentage of their maximal muscle exertion to execute a task with the same posture and applied external force as humans.

Previous *in vitro* research on chimpanzees has shown them to have a greater absolute PCSA than humans for all muscles in the present glenohumeral model. Even when scaled to the same body mass, chimpanzees still have greater relative PCSA across all muscles (Table 1) (Thorpe et al., 1999). There are notable muscles with a PCSA that are much greater than the human muscle PCSA. These included the coracobrachialis, middle deltoid, subscapularis and supraspinatus. Increased PCSA increases the force production capabilities of a muscle by increasing muscle fiber content (Nigg and Herzog, 2007). That shoulder muscles in chimpanzees have a PCSA greater than that of humans demonstrates a large difference in force production capabilities between species (Thorpe et al., 1999). The most pronounced differences in PCSA may indicate the heightened importance of the subscapularis, supraspinatus and middle deltoid in producing rotational and stabilizing forces about the shoulder and glenohumeral joint in particular.

At the rotator cuff, muscular contribution from subscapularis and supraspinatus was almost exclusively only predicted in the chimpanzee glenohumeral model. While chimpanzees generally have a greater overall muscle mass and relative PCSA in their upper extremity than humans, the difference between species in each individual muscle also varies (Sonnabend and Young, 2009). Because of a wide breadth of upper extremity-inclusive locomotor behaviors, primates, including humans and chimpanzees, typically have a 'subscapularis dominant' rotator cuff (Mathewson et al., 2014). Yet, the human supraspinatus and subscapularis are relatively smaller than those of other primates that habitually use their upper extremity in a climbing or suspensory capacity (Inman et al., 1944; Larson, 2015; Mathewson et al., 2014; Sonnabend and Young, 2009). The greater absolute and relative PCSA of the chimpanzee supraspinatus and subscapularis indicates a greater capacity for producing forces to stabilize the glenohumeral joint (Larson and Stern, 1986). The smaller size of the human supraspinatus and subscapularis may have made the human shoulder less idealized for the strenuous tasks of climbing and suspension, and thus weak mechanical contributors.

Less multi-muscle contribution in the computational predictions of the rotator cuff could represent biological unsustainability of weight-bearing suspension and climbing in humans. Both the subscapularis and infraspinatus exert an inferior pull about the glenohumeral joint in chimpanzees and humans, countering the superior action of the deltoids and supraspinatus in many postures (Inman et al., 1944; Roberts, 1974), and maintaining the width of the subacromial space. It is surprising that the supraspinatus was not active in the human model. The supraspinatus is generally active during overhead activities to elevate the arm in synergy with the deltoids (Inman et al., 1944). As a result of the use of an optimization routine to predict muscle forces, the greater force-producing capacity of the deltoids was likely selected over the small supraspinatus in the human model to provide the required superior force. Unlike habitually climbing and suspensory chimpanzees, the entire modern human rotator cuff has evolved to be small, to reduce segment mass and inertial properties for increasingly non-weight-

bearing behaviors that require less muscular effort (Larson et al., 2000; Raichlen, 2006; Schoonaert et al., 2007; Taylor et al., 1974). This has allowed a more energy efficient redirection of muscular effort toward non-locomotor modern behaviors, particularly those below shoulder height, such as tool making and manipulating, and hunting and throwing (Arias-Martorell, 2019; Mathewson et al., 2014; Roach et al., 2013; Sonnabend and Young, 2009; Young et al., 2015). As the subscapularis is particularly reduced in size and weakened in humans (Mathewson et al., 2014), the infraspinatus is the primary preventative means to superior migration of the humeral head and reduction of the subacromial space. The human model predicted high muscle forces from the infraspinatus to provide inferior forces about the glenohumeral joint, a scenario that would accelerate infraspinatus fatigue. Along with superior humeral head migration, fatigue of the infraspinatus can reduce the posterior tilt and lateral rotation of the scapula necessary to widen the subacromial space in overhead postures (Borstad et al., 2009; Ebaugh et al., 2006b; Tsai et al., 2003). As chimpanzees have a large infraspinatus and subscapularis, in part to counter deltoid action, this may guard against overload of a single muscle, as was predicted in the model.

Model-predicted activation of the deltoids differed between species in both amplitude and timing. The deltoids are active during the support phase in experimental studies on chimpanzees and humans, to raise the arm and counter traction at the glenohumeral joint from hanging and suspension (Larson and Stern, 1986; MacLean and Dickerson, 2019). Humans were predicted to activate all three deltoids to a much higher degree than chimpanzees. Chimpanzees have greater force-producing capacity in their upper extremity muscles than humans, including the deltoids, and lower body mass (Thorpe et al., 1999; Walker, 2009). As such, a lower percentage of their musculature was predicted to complete the same postural task as humans. The chimpanzee model predicted no contribution from the anterior deltoid in support phase, whereas the human model predicted the greatest contribution from the anterior deltoid. This may be due to differences in muscle lines of action, as computational models and optimization routines are often very sensitive to variation in muscle lines of action and subsequently selective about which muscles are active in specific postures (Latash, 2012; Nussbaum and Chaffin, 1996). Given the broad base of origin of the deltoid across the scapula and clavicle (Inman et al., 1944), the modeled anterior deltoid line of action was likely positioned as the most efficient prime mover in the human model for producing a superior force at the glenohumeral joint. The greater predicted activation of all three deltoids in humans could have repercussions for shoulder function, as activation of arm abductors decreases the subacromial space (Graichen et al., 2001).

Between-species glenohumeral geometry

The subacromial space was wider at all static instances of the suspension cycle in the chimpanzee model, a possible geometric mechanism for reduced subacromial impingement risk in the species. The difference between species was approximately 2 mm throughout the entire suspension cycle. The laterally projecting human acromion is typically sloped inferiorly, unlike in chimpanzees, which can reduce the width of the subacromional space across most postures (Voisin et al., 2014). The increased space between the humerus and acromion in chimpanzees would provide a wider berth for tissues in the subacromial space, such as the supraspinatus, throughout the range of shoulder elevation, reducing the risk for impingement of tissues (Lewis et al., 2001). While the reduction in size and absolute PCSA of the supraspinatus in humans brought about decreases in force production, it is likely related to the need to exist in a narrower subacromial space (Voisin et al., 2014).

Differences between species in the subacromial space are partly the result of geometric changes in scapular bone shape. Chimpanzees have a more superiorly oriented glenoid, scapular spine and acromion. This reorients the lines of action of the deltoids and rotator cuff to optimize overhead behaviors, particularly propulsive arm swinging motions (Larson, 2007; Larson and Stern, 1986; Roach et al., 2013). Humans have a laterally oriented glenoid, scapular spine and acromion. Humans also have an enlarged and widened acromion process, and lateral projection of the acromion over the glenohumeral joint (Schultz, 1968; Voisin et al., 2014). The laterally oriented human glenoid establishes the human range of motion as ideal for the use of the hands in front of the body and below the shoulder, while also optimizing the glenohumeral muscle lines of action for lateral motions such as throwing (Larson, 1988; Roach et al., 2013). The lateral projection of the acromion changes the mechanical leverage of the deltoids, shifting the muscle origin to be over the joint. This improves the deltoid moment arm in below-the-shoulder action and compensates for the reduced force production of the supraspinatus muscle (Lewis et al., 2001; Voisin et al., 2014). However, the lateral orientation and projection of the acromion also reduces the subacromial space, resulting in higher injury risk for impingement in humans (Lewis et al., 2001; Voisin et al., 2014).

Effect of musculoskeletal differences on function

The driving forces behind and stages of evolutionary change in the human subacromial space and rotator cuff, and the propensity for rotator cuff pathology remain unclear. Tissue mass and shape are modified by external stimuli and loading (Byron et al., 2011; Green et al., 2012; Robling et al., 2006; Ruff et al., 2006; Turner, 2007). Scapular shape and rotator cuff muscle mass and PCSA are influenced by exposure to the external forces experienced through typical upper extremity behaviors. Therefore, evolutionary adaptations to scapular shape and rotator cuff architecture have occurred in conjunction with evolutionary behavioral modifications. The increasing need to walk bipedally, hunt or throw were likely strong influences on the lateralization of the scapula (Larson, 2007; Lewis et al., 2001; Roach et al., 2013). Unlike arboreal behaviors, these behaviors maintain below-shoulder multiplanar ranges of motion. It has been hypothesized that the acromion became more lateralized to optimize leverage of the deltoids for below-shoulder behaviors, leading to a lowered mass and PCSA of the supraspinatus tendon (Voisin et al., 2014). This theory may imply that scapular shape adaptations toward modern human behaviors precede adaptations in rotator cuff muscle size and PCSA. However, these changes may have been simultaneous. Concurrent with increasing bipedalism, a parallel reduction in arborealism would have reduced the external forces on the shoulder from locomotion. Increasingly less arborealism would reduce the necessary contribution of the rotator cuff to the repetitive or sustained force-producing arm elevation and axial rotation (Larson and Stern, 2013; Larson, 2015; Sonnabend and Young, 2009). These beneficial evolutionary adaptations optimized the human shoulder for evolutionarily advantageous behaviors such as walking, throwing and tool manipulation, but consequently may have resulted in negative vestigial consequences, particularly for the modern, industrialized human existence.

Relative to the musculoskeletal diversity of life, small differences between closely related species in bone shape and orientation can greatly affect joint function and pathology. All primates share a similar shoulder organization (Pronk, 1991; Sonnabend and Young,

2009). While modern human climbing and overhead capacity is still present, it is greatly reduced compared with that of other primates as a result of these adaptations to the shoulder complex. The rotator cuff and deltoids form a series of force couples around the glenohumeral joint that act to center the humeral head in the glenoid (Larson and Stern, 1986). The superior unit of the force couples is composed of the deltoids and supraspinatus, which elevate the arm, while the inferior unit is composed of the rest of the rotator cuff, which depresses the arm (Inman et al., 1944). The reduced force-producing capability of the subscapularis in humans represents an evolutionary adaptation that has reduced its contribution to centering the humeral head in the glenoid against the superior pull of the deltoids (Potau et al., 2009). This has increased the susceptibility of humeral head superior migration and subsequent subacromial space impingement. Deleterious consequences of superior migration of the humeral head in humans are compounded by the more lateral projection of the acromion over the humeral head and the less superior orientation of the acromion (Larson, 2007; Voisin et al., 2014). Combined, the reduced PCSA, altered scapular shape and composition of the rotator cuff and deltoids may be evolutionary indications of why humans have a propensity for subacromial impingement syndrome that does not exist in other primates.

Alternatively, the primate shoulder, and the shoulder of some extinct hominin species, has protective musculoskeletal mechanisms in the musculoskeletal morphology of the rotator cuff and scapula. If both humans and chimpanzees have evolved from an arboreal common ancestor, chimpanzees have retained the capability and musculoskeletal system necessary for these behaviors. With more massive rotator cuff muscles, the ratio of the deltoid muscle group to the rotator cuff is closer to 1:1 in chimpanzees. This ensures the rotator cuff can counter the superior pull of the deltoids in arm elevation without the risk of early-onset fatigue that would alter glenohumeral biomechanics during high force upper extremity arboreal behaviors. Chimpanzees also retain a superiorly oriented scapular spine and acromion, and an acromion process that does not project as laterally as that of humans (Voisin et al., 2014). This has widened the subacromial space and reduced the area over which the acromion can impinge the supraspinatus over the humeral head. Chimpanzees resultantly have evolved protection against subacromial impingement syndrome and rotator cuff pathology (Lewis et al., 2001). While there is limited information on extant hominin muscle architecture, australopithecines appear to have a scapular spine that falls between the superior orientation of a chimpanzee and the lateral orientation of a modern human scapular spine (Haile-Selassie et al., 2010). *Australopithecus afarensis* is believed to be bipedal based upon lower extremity morphology, with an upper extremity that may still have engaged in climbing (Crompton et al., 1998; Haile-Selassie et al., 2010; Green and Alemseged, 2012). The intermediate scapular spine orientation of *Australopithecus afarensis* would reduce the width and occupational ratio of the subacromial space. Therefore, either the rotator cuff was already becoming smaller to occupy a smaller subacromial space or there was incongruency between the size of the supraspinatus and the subacromial space. Either scenario would indicate the possible mild beginnings of reduced arboreal capacity and increased risk of rotator cuff pathology in *Australopithecus afarensis*, indicative of the slow adaptation away from arborealism in the human evolutionary tree.

Limitations and future directions

A series of assumptions and limitations accompanied the development of the chimpanzee glenohumeral model and the computational comparison between humans and chimpanzees. Many of these decisions stemmed from the unavailability of desirable relevant datasets, but can be modified in future model iterations. While computational musculoskeletal modeling offers numerous benefits to biomechanical studies of the human body, several limitations constrain the present modeling of the glenohumeral joint. The shoulder is considered a three-joint structure, and the acromioclavicular and sternothoracic joints were not considered, though the torso and clavicle were geometrically positioned to dictate the position of the scapula and influence shoulder rhythm (Voisin, 2006). Soft tissue mechanics were simplified in the study to muscle mass and PCSA. Ligaments were set as inactive in both models, and did not contribute to joint stability. Additionally, optimization routines, as used in the glenohumeral model, may overlook the contribution of small muscles to a task in favor of larger muscles with greater force-producing capabilities (Dickerson et al., 2007), reducing synergistic muscle recruitment. Computation musculoskeletal modeling is limited by how researchers can mathematically represent biological phenomena. To model the entirety of the human musculoskeletal system is computationally expensive and often leads to more assumptions, difficulty in interpretation and erroneous results (Cholewicki et al., 1995). Assumptions are crucial in producing models that adequately address the primary research questions at hand. The present model aimed to compare the glenohumeral musculoskeletal behaviors between two species, particularly differences in muscle patterns and overall usage. The models are considered to have achieved this purpose.

The postural analysis run in the present study did not replicate the full breadth of differences between chimpanzees and humans. The kinematic inputs for the chimpanzee model derived from human experimentation. This would have reduced the realism of the joint center positions, subacromial space width and joint angle decomposition. However, if the kinematic inputs are not representative of a chimpanzee suspension kinematics, then the identification of differences stemming from this comparison between species are likely conservative. The model was run statically, not dynamically. This negated the effect of motion and momentum, which would influence joint forces, and muscular recruitment patterns in a powerful and propulsive behavior such as brachiation (Larson and Stern, 1986). Assumptions were made about hand force in each of the support phase static instances. For the initial static analysis, whole or half body mass operated as a provisional representative of hand force in the three support phase discrete instances of the horizontal bimanual arm suspension cycle and in the direction of gravitational force only. This approach disregarded the multidimensional effect of the hand forces at the handhold. A static analysis was considered the most appropriate initial analysis to make comparisons between species in glenohumeral function, given the complications of assumptions required for dynamic modeling of the suspension cycle in the absence of high-quality chimpanzee kinematic data. The models are both capable of running dynamic assessments of climbing and suspension for future study.

The models are both limited by the choice of individual and musculoskeletal data used to represent each species. Each model was run using postural, anthropometric, task-specific inputs from a single, average individual. As well, the geometry module of both models used bone scan inputs from a single, different individual. Other musculoskeletal features and parameters, such as segment parameters, muscle PCSA, origins and insertions, relied on collected and dissected mean data from a variety of published

Journal of Experimental Biology (2020) 223, jeb225987. doi:10.1242/jeb.225987

databases. The choice of these single or mean inputs influenced the results. However, as each of these single inputs or model parameters was selected to represent an average chimpanzee or human, the results as presented provide an initial view of the differential musculoskeletal model outputs. The model can run multiple subject inputs when available, or be run probabilistically through appropriate software, to give better population level predictions. As large variability exists in both kinematics and bone geometry of both species, each model is limited by how much the motion data and musculoskeletal geometry represent an average individual. There is limited data on chimpanzees, however, so the data utilized in the present study represented the best available options. Should improved musculoskeletal or motion data become available, both models would be highly receptive of new modular parameters.

Unique assumptions related to chimpanzee musculoskeletal behavior were incorporated into the creation of the chimpanzee model, owing once more to limited data on chimpanzees. The

Table 3. List of the current design of the chimpanzee model inputs as well as internal model parameters, the assumptions and limitations of each in its current iteration, and possible improvements for future analyses

Chimpanzee model input or parameter	Current iteration	Assumption(s)	Limitation(s)	Future implementations
Motion data inputs	Modified human data No direct kinematic data available	Chimpanzee upper extremity kinematics similar to human	Not chimpanzee kinematic data	Acquire chimpanzee kinematic data Multi-subject analysis
Anthropometric inputs	A single average subject	Representative of average chimpanzee	Single-subject representation	Multi-subject/probabilistic analysis
Task-specific inputs	Assumed hand forces in the direction of gravity only No direct data available	Values represent true suspension hand forces	Not a direct measure Disregards 3D applied forces at the hand Single-subject representation	Acquire hand forces Multi-subject/probabilistic analysis
Bone scans	MRI images of single chimpanzee	Representative of average chimpanzee	Single-subject representation	Multi-subject/probabilistic analysis
Shoulder rhythm	Developed computationally with x-rays Uses modified human kinematic data No shoulder rhythm data currently available	3D bone positions can be determined from x-rays Chimpanzee 3D bone positions can be determined with modified human kinematic inputs Mean values from equations representative of chimpanzees	3D positioning with 2D static x-rays x-ray arm positions in limited range of motion Human kinematics affect scapular, clavicular and humeral position Mean regression equations do not represent variability	Develop rhythm computationally with chimpanzee kinematic inputs, and/or 3D scans in large arm range of motion Or retrieve scapular and clavicular orientations through experimental analysis
Muscle origins and insertions	Placement using published muscle footprints 3D positions not available	Manual placement at centroid of footprint	Placement may not be best representation of origin or insertion	Obtain 3D placements
Muscle lines of action	Assumed best placement between origin and insertion No direct data available	Lines of action will follow direct wrapping from origin to insertion	Lines of action may have more complex paths	Acquire direct lines of action data
Ligaments	Set as inactive No ligamentous force or origin and insertion data available	Ligamentous contribution can be omitted	Omits contribution of ligaments to joint stability	Acquire data on ligament contribution to joint stability
PCSA	Retrieved from published sources	Single values representative of an average chimpanzee Infraspinatus/subscapularis muscle element ratios assumed to match human	Not representative of range of possible values Infraspinatus/subscapularis element PCSA likely different from human	Measure muscle element PCSA for infraspinatus and subscapularis Multi-subject/probabilistic analysis
Specific tension	Same single value as in human model No direct data available	Same value for all muscles Same values as humans	Not chimpanzee specific tension values	Acquire chimpanzee specific tension values for each muscle, or a single representative value
Glenohumeral stability ratios	Modified human stability ratios based on species differences in glenoid depth No direct data available	Species differences in directional stability ratios are only due to glenoid depth	Chimpanzee glenohumeral joint stability may be directionally different	Acquire *in vitro* chimpanzee analysis of glenohumeral directional stability ratios

shoulder rhythm algorithms were adapted from a previously developed human shoulder rhythm and used two-dimensional x-rays to define modified chimpanzee scapular and clavicular orientations. The limited postures of the chimpanzees in these x-rays likely affected the approximated boney orientations and resulting shoulder rhythm, particularly the anterior/posterior tilt. This may have also affected the realism of the subacromial space width predictions. Scapulothoracic contact force application sites, joint centers and glenohumeral contact force constraints were estimated from regression equations designed for the human upper extremity. Specific tension was assumed to be equivalent to human estimates. The paucity of complete information required considerable flexibility, experimentation and adaptability during the construction of this model. However, the model was created to enable efficient algorithm adjustment based on alternative hypotheses, and to allow modifications as novel future musculoskeletal and kinematic data on chimpanzees arise. The very existence of the initial exploratory model is imperative for progress and the success of future studies on primate evolutionary shoulder function.

The novel chimpanzee model is designed for a specific use and contains a series of biomechanical and physiological assumptions, both of which must be considered when interpreting results. This model is intended for comparative analyses with other species models only. It is not meant to be a standalone model to predict chimpanzee musculoskeletal shoulder behavior. Rather, the model is designed to run concurrently with a parallel model, to provide insight into differences between species in musculoskeletal function in analogous computational environments and conditions. These musculoskeletal outputs can include muscle moment arms, muscle patterns and coordination, and joint kinetics and stability for any upper extremity task. The model utilizes kinematic, anthropometric and task-specific inputs and any interpretation of comparative model results are limited by the quality of these inputs, particularly kinematic inputs. The model is designed with specific internal settings, and the outputs are also dependent on the quality of these parameters. These factors have been outlined in Table 3 to elucidate the limitations of the model in its current form and how improvements can be implemented should new chimpanzee data become available.

The model can be used to test additional specific, comparative hypotheses through further analyses. The chimpanzee glenohumeral model does not represent a substitution for *in vivo* and *in vitro* evolutionary and comparative studies. Rather, the model serves as an alternative method of analysis for testing a variety of musculoskeletal computational 'what if' scenarios that may be difficult to test morphometrically or experimentally (Hutchinson, 2012). Hypotheses that can be tested with comparative models include between-species differences in muscle coordination and contribution, subacromial space width, joint stability, and joint forces and moments. Many specific hypotheses can be tested using the model by modifying inputs and internal model parameters. Future analyses can test different inputs, including motion data, anthropometrics and task-specific inputs. Additional upper extremity behaviors that may be valuable to analyze computationally could include different throwing techniques, reaching and arm swing during gait. Internal model parameters can also be modified to test other comparative hypotheses. Different bone scans, PCSA values, muscle origins and insertions, shoulder rhythm equations or glenohumeral stability ratios can be applied to test the effect of these geometric musculoskeletal settings on musculoskeletal outputs. Finally, performing multi-subject analyses using multiple matching kinematic, anthropometric and task-specific inputs will provide data samples for greater population-level comparative analyses. Alternatively, probabilistic analyses can be applied to both model inputs to assess functional variability between species, and model parameters such as PCSA, bone shape and lines of action to assess functional sensitivity (Langenderfer et al., 2008; Chopp-Hurley et al., 2014).

Conclusion

While prevalent in biomechanics and engineering, computational modeling is still recent and largely unexplored in evolutionary science. Classical measuring techniques in physical anthropology have limitations that may discount the manner in which features of the musculoskeletal form operate synergistically within a complex mechanical system (Hutchinson, 2012). Computational models such as the presently developed chimpanzee model allow assessment of specific features of the musculoskeletal system, and how they interact to produce strategies for movement at the shoulder. Primate computational models provide benefits to exploring and answering evolutionary, fundamental physiological and biomechanical, and modern human functional questions. Understanding evolutionary adaptations of the modern human shoulder can aid our understanding of specific strengths and weaknesses of the modern shoulder, the root causes of injury risk, and how to avoid them.

The present results confirm that while chimpanzees and humans have very similar gross musculoskeletal anatomy, changes to the musculoskeletal system have influenced muscle force production in overhead postures. The laterally orientated glenoid and laterally oriented and projected acromion have narrowed the human subacromial space. The reduced PCSA of many muscles crossing the human glenohumeral joint have modified joint stabilizing force couples. As a result, muscles like the infraspinatus may be overloaded and highly susceptible to fatigue in overhead postures. These adaptations have enabled essential modern human behaviors, but may also explain the modern human propensity for subacromial impingement and rotator cuff tears.

Acknowledgements

The authors would like to acknowledge the contribution of Dr Susan Larson (Stony Brook University), Dr Nathan Thompson (New York Institute of Technology), Dr Brian Umberger (University of Michigan) and Dr Matthew O'Neill (Midwestern University), for providing chimpanzee EMG, x-ray and skeletal data, respectively, which greatly helped in the development and evaluation of the chimpanzee model. Some results, figure legends and discussion in this paper are reproduced from the PhD thesis of Kathleen MacLean (MacLean, 2018).

Competing interests

The authors declare no competing or financial interests.

Author contributions

Conceptualization: K.F.M., C.R.D.; Methodology: K.F.M., C.R.D.; Software: K.F.M., C.R.D.; Validation: K.F.M., C.R.D.; Formal analysis: K.F.M.; Investigation: K.F.M.; Resources: K.F.M., C.R.D.; Data curation: K.F.M.; Writing - original draft: K.F.M.; Writing - review & editing: K.F.M., C.R.D.; Visualization: K.F.M.; Supervision: C.R.D.; Project administration: K.F.M., C.R.D.; Funding acquisition: C.R.D.

Funding

This research was partially funded with combined support from a Natural Sciences and Engineering Research Council of Canada Discovery Grant to C.R.D. (311895-2016) and a Canada Research Chairs grant in Shoulder Mechanics to C.R.D.

References

Arias-Martorell, J. (2019). The morphology and evolutionary history of the glenohumeral joint of hominoids: a review. *Ecol. Evol.* **9**, 703-722. doi:10.1002/ece3.4392

Ashton, E. H. and Oxnard, C. E. (1963). The musculature of the primate shoulder. *Trans. Zool. Soc. Lond.* **29**, 553-650. doi:10.1111/j.1096-3642.1963.tb00222.x

Ashton, E. H., Flinn, R. M., Oxnard, C. E. and Spence, T. F. (1976). The adaptive and classificatory significance of certain quantitative features of the forelimb in primates. *J. Zool.* **179**, 515-556. doi:10.1111/j.1469-7998.1976.tb02309.x

Basmajian, J. V. and De Luca, C. J. (1985). *Muscles Alive*, 5th edn. Baltimore, Maryland: Williams & Wilkins.

Bertram, J. E. A. and Chang, Y.-H. (2001). Mechanical energy oscillations of two brachiation gaits: measurement and simulation. *Am. J. Phys. Anthropol.* **115**, 319-326. doi:10.1002/ajpa.1088

Bey, M. J., Brock, S. K., Beierwaltes, W. N., Zauel, R., Kolowich, P. A. and Lock, T. R. (2007). In vivo measurement of subacromial space width during shoulder elevation: technique and preliminary results in patients following unilateral rotator cuff repair. *Clin. Biomech.* **22**, 767-773. doi:10.1016/j.clinbiomech.2007.04.006

Borstad, J. D., Szucs, K. and Navalgund, A. (2009). Scapula kinematic alterations following a modified push-up plus task. *Hum. Mov. Sci.* **28**, 738-751. doi:10.1016/j.humov.2009.05.002

Buchanan, T. S., Lloyd, D. G., Manal, K. and Besier, T. F. (2004). Neuromusculoskeletal modeling: estimation of muscle forces and joint moments and movements from measurements of neural command. *J. Appl. Biomech.* **20**, 367-395. doi:10.1123/jab.20.4.367

Byron, C., Kunz, H., Matuszek, H., Lewis, S. and Van Valkinburgh, D. (2011). Rudimentary pedal grasping in mice and implications for terminal branch arboreal quadrupedalism. *J. Morphol.* **272**, 230-240. doi:10.1002/jmor.10909

Carlson, K. J. (2006). Muscle architecture of the common chimpanzee (*Pan* troglodytes): perspectives for investigating chimpanzee behavior. *Primates* **47**, 218-229. doi:10.1007/s10329-005-0166-4

Cartmill, M. and Smith, F. H. (2009). *The Human Lineage*. Hoboken, New Jersey: John Wiley & Sons, Inc.

Chaffin, D. B. (1997). Development of computerized human static strength simulation model for job design. *Hum. Factors Ergonomic Manufactur.* **7**, 305-322. doi:10.1002/(SICI)1520-6564(199723)7:4<305::AID-HFM3>3.0.CO;2-7

Cholewicki, J., McGill, S. M. and Norman, R. W. (1995). Comparison of muscle forces and joint load from an optimization and EMG assisted lumbar spine model: towards development of a hybrid approach. *J. Biomech.* **28**, 321-331. doi:10.1016/0021-9290(94)00065-C

Chopp, J. N., O'Neill, J. M., Hurley, K. and Dickerson, C. R. (2010). Superior humeral head migration occurs after a protocol designed to fatigue the rotator cuff: a radiographic analysis. *J. Shoulder Elbow Surg.* **19**, 1137-1144. doi:10.1016/j.jse.2010.03.017

Chopp-Hurley, J. N., Langenderfer, J. E. and Dickerson, C. R. (2014). Probabilistic evaluation of predicted force sensitivity to muscle attachment and glenohumeral stability uncertainty. *Ann. Biomed. Eng.* **42**, 1867-1879. doi:10.1007/s10439-014-1035-3

Collard, M. and Wood, B. (2000). How reliable are human phylogenetic hypotheses? *Proc. Natl Acad. Sci. USA* **97**, 5003-5006. doi:10.1073/pnas.97.9.5003

Cote, M. P., Gomlinski, G., Tracy, J. and Mazzocca, A. D. (2009). Radiographic analysis of commonly prescribed scapular exercises. *J. Shoulder Elbow Surg.* **18**, 311-316. doi:10.1016/j.jse.2008.09.010

Crompton, R. H., Weijie, L. Y. W., Günther, M. M. and Savage, R. (1998). The mechanical effectiveness of erect and "bent-hip, bent-knee" bipedal walking in Australopithecus afarensis. *J. Hum. Evol.* **35**, 55-74. doi:10.1006/jhev.1998.0222

De Luca, C. J. (1997). The use of surface electromyography in biomechanics. *J. Appl. Biomech.* **13**, 135-163. doi:10.1123/jab.13.2.135

Demes, B. and Carlson, K. J. (2009). Locomotor variation and bending regimes of capuchin limb bones. *Am. J. Phys. Anthropol.* **139**, 558-571. doi:10.1002/ajpa.21020

Dickerson, C. R. (2005). A biomechanical analysis of shoulder loading and effort during load transfer tasks. *Thesis Dissertation*. University of Michigan. Ann Arbor, Michigan.

Dickerson, C. R., Chaffin, D. B. and Hughes, R. E. (2007). A mathematical musculoskeletal shoulder model for proactive ergonomic analysis. *Comput. Methods Biomech. Biomed. Engin.* **10**, 389-400. doi:10.1080/10255840701592727

Dickerson, C. R., Hughes, R. E. and Chaffin, D. B. (2008). Experimental evaluation of a computational shoulder musculoskeletal model. *Clin. Biomech.* **23**, 886-894. doi:10.1016/j.clinbiomech.2008.04.004

Dickerson, C. R., Meszaros, K. A., Cudlip, A. C., Chopp-Hurley, J. N. and Langenderfer, J. E. (2015). The influence of cycle time on shoulder fatigue responses for a fixed total overhead workload. *J. Biomech.* **48**, 2911-2918. doi:10.1016/j.jbiomech.2015.04.043

Diogo, R., Potau, J. M. and Pastor, J. F. (2013). *Photographic and Descriptive Musculoskeletal Atlas of Chimpanzees: With Notes on the Attachments, Variations, Innervation, Function and Synonymy and Weight of the Muscles*, 1st edn. New York, USA: CRC Press, Taylor & Francis Group.

Dul, J., Townsend, M. A., Shiavi, R. and Johnson, G. E. (1984). Muscular synergism—I. On criteria for load sharing between synergistic muscles. *J. Biomech.* **17**, 663-673. doi:10.1016/0021-9290(84)90120-9

Ebaugh, D. D., McClure, P. W. and Karduna, A. R. (2006a). Effects of shoulder muscle fatigue caused by repetitive overhead activities on scapulothoracic and glenohumeral kinematics. *J. Electromyogr. Kinesiol.* **16**, 224-235. doi:10.1016/j.jelekin.2005.06.015

Ebaugh, D. D., McClure, P. W. and Karduna, A. R. (2006b). Scapulothoracic and glenohumeral kinematics following an external rotation fatigue protocol. *J. Orthop. Sports Phys. Ther.* **36**, 557-571. doi:10.2519/jospt.2006.2189

Folkl, A. K. (2013). Characterizing the consequences of chronic climbing-related injury in sport climbers and boulderers. *Wilderness Environ. Med.* **24**, 153-158. doi:10.1016/j.wem.2012.11.010

Garner, B. A. and Pandy, M. G. (2001). Musculoskeletal model of the upper limb based on the visible human male dataset. *Comput. Methods Biomech. Biomed. Engin.* **4**, 93-126. doi:10.1080/10255840008908000

Graichen, H., Stammberger, T., Bonél, H., Wiedemann, E., Englmeier, K.-H., Reiser, M. and Eckstein, F. (2001). Three-dimensional analysis of shoulder girdle and supraspinatus motion patterns in patients with impingement syndrome. *J. Orthop. Res.* **19**, 1192-1198. doi:10.1016/S0736-0266(01)00035-3

Green, D. J. and Alemseged, Z. (2012). Australopithecus afarensis scapular ontogeny, function, and the role of climbing in human evolution. *Science* **338**, 514-517. doi:10.1126/science.1227123

Green, D. J., Richmond, B. G. and Miran, S. L. (2012). Mouse shoulder morphology responds to locomotor activity and the kinematic differences of climbing and running. *J. Exp. Zool. B* **318**, 621-638. doi:10.1002/jez.b.22466

Grewal, T.-J. and Dickerson, C. R. (2013). A novel three-dimensional shoulder rhythm definition that includes overhead and axially rotated humeral postures. *J. Biomech.* **46**, 608-611. doi:10.1016/j.jbiomech.2012.09.028

Grewal, T.-J., Cudlip, A. C. and Dickerson, C. R. (2017). Comparing non-invasive scapular tracking methods across elevation angles, planes of elevation and humeral axial rotations. *J. Electromyogr. Kinesiol.* **37**, 101-107. doi:10.1016/j.jelekin.2017.10.001

Grieve, J. R. and Dickerson, C. R. (2008). Overhead work: Identification of evidence-based exposure guidelines. *Occup. Erg.* **8**, 53-66.

Haile-Selassie, Y., Latimer, B. M., Alene, M., Deino, A. L., Gibert, L., Melillo, S. M., Saylor, B. Z., Scott, G. R. and Lovejoy, C. O. (2010). An early Australopithecus afarensis postcranium from Woranso-Mille, Ethiopia. *Proc. Natl Acad. Sci. USA* **107**, 12121-12126. doi:10.1073/pnas.1004527107

Högfors, C., Peterson, B., Sigholm, G. and Herberts, P. (1991). Biomechanical Model of the Human Shoulder-II. The Shoulder Rhythm. *J. Biomech.* **24**, 699-709. doi:10.1016/0021-9290(91)90334-J

Hutchinson, J. R. (2012). On the inference of function from structure using biomechanical modelling and simulation of extinct organisms. *Biol. Lett.* **8**, 115-118. doi:10.1098/rsbl.2011.0399

Inman, V. T., Saunders, J. B. C. M. and Abbott, L. C. (1944). Observations of the function of the shoulder joint. *J. Bone Joint Surg.* **26**, 1-30.

Karduna, A. R., McClure, P. W., Michener, L. A. and Sennett, B. (2001). Dynamic measurements of three-dimensional scapular kinematics: a validation study. *J. Biomech. Eng.* **123**, 184-190. doi:10.1115/1.1351892

Kikuchi, Y. (2010). Comparative analysis of muscle architecture in primate arm and forearm. *J. Vet. Med.* **39**, 93-106. doi:10.1111/j.1439-0264.2009.00986.x

Kivell, T. L. and Schmitt, D. (2009). Independent evolution of knuckle-walking in African apes shows that humans did not evolve from a knuckle-walking ancestor. *Proc. Natl. Acad. Sci. USA.* **106**, 14241-14246. doi:10.1073/pnas.0901280106

Langenderfer, J. E., Laz, P. J., Petrella, A. J. and Rullkoetter, P. J. (2008). An efficient probabilistic methodology for incorporating uncertainty in body segment parameters and anatomical landmarks in joint loadings estimated from inverse dynamics. *J. Biomech. Eng.* **130**, 014502. doi:10.1115/1.2838037

Larson, S. G. (1988). Subscapularis function in gibbons and chimpanzees: implications for interpretation of humeral head torsion in hominoids. *Am. J. Phys. Anthropol.* **76**, 449-462. doi:10.1002/ajpa.1330760405

Larson, S. G. (1998). Parallel evolution in the hominoid trunk and forelimb. *Evol. Anthropol.: Issues New Rev.* **6**, 87-99. doi:10.1002/(SICI)1520-6505(1998)6:3<87::AID-EVAN3>3.0.CO;2-T

Larson, S. G. (2007). Evolutionary transformation of the hominin shoulder. *Evol. Anthropol. Issues New Rev.* **16**, 172-187. doi:10.1002/evan.20149

Larson, S. G. (2015). Rotator cuff muscle size and the interpretation of scapular shape in primates. *J. Hum. Evol.* **80**, 96-106. doi:10.1016/j.jhevol.2015.01.001

Larson, S. G. and Stern, J. T., Jr. (1986). EMG of scapulohumeral muscles in the chimpanzee during reaching and "arboreal" locomotion. *Am. J. Anat.* **276**, 171-190. doi:10.1002/aja.1001760207

Larson, S. G. and Stern, J. T., Jr. (1992). Further evidence for the role of supraspinatus in quadrupedal monkeys. *Am. J. Phys. Anthropol.* **87**, 359-363. doi:10.1002/ajpa.1330870310

Larson, S. G. and Stern, J. T., Jr. (2013). Rotator cuff muscle function and its relation to scapular morphology in apes. *J. Hum. Evol.* **65**, 391-403. doi:10.1016/j.jhevol.2013.07.010

Larson, S. G., Stern, J. T., Jr and Jungers, W. L. (1991). EMG of serratus anterior and trapezius in the chimpanzee: scapular rotators revisited. *Am. J. Phys. Anthropol.* **85**, 71-84. doi:10.1002/ajpa.1330850109

Larson, S. G., Schmitt, D., Lemelin, P. and Hamrick, M. (2000). Uniqueness of primate forelimb posture during quadrupedal locomotion. *Am. J. Phys. Anthropol.* **112**, 87-101. doi:10.1002/(SICI)1096-8644(200005)112:1<87::AID-AJPA9>3.0.CO;2-B

Latash, M. L. (2012). The bliss (not the problem) of motor abundance (not redundancy). *Exp. Brain Res.* **217**, 1-5. doi:10.1007/s00221-012-3000-4
Lewis, J., Green, A., Yizhat, Z. and Pennington, D. (2001). Subacromial impingement syndrome. Has Evolution failed us? *Physiotherapy* **87**, 191-198. doi:10.1016/S0031-9406(05)60605-0
Lippitt, S. B., Vanderhooft, J. E., Harris, S. L., Sidles, J. A., Harryman, D. T. and Matsen, F. A. (1993). Glenohumeral stability from concavity-compression: a quantitative analysis. *J. Shoulder Elbow Surg.* **2**, 27-35. doi:10.1016/S1058-2746(09)80134-1
Lovejoy, C. O., Suwa, G., Simpson, S. W., Matternes, J. H. and White, T. D. (2009). The great divides: Ardipithecus ramidus reveals the postcrania of our last common ancestors with African apes. *Science* **326**, 100-106.
Ludewig, P. M. and Cook, T. M. (2000). Alterations in shoulder kinematics and associated muscle activity in people with symptoms of shoulder impingement. *Phys. Ther.* **80**, 276-291. doi:10.1093/ptj/80.3.276
Ludewig, P. M., Phadke, V., Braman, J. P., Hassett, D. R., Cieminski, C. J. and LaPrade, R. F. (2009). Motion of the shoulder complex during multiplanar humeral elevation. *J. Bone Joint Surg.* **91**, 378-389. doi:10.2106/JBJS.G.01483
Macias, M. E. and Churchill, S. E. (2015). Functional morphology of the neandertal scapular glenoid fossa. *Anat. Rec.* **298**, 168-179. doi:10.1002/ar.23072
MacLean, K. (2018). Development of a probablistic chimpanzee glenohumeral model: implications for human function. PhD thesis, University of Waterloo, ON, Canada.
MacLean, K. F. E. and Dickerson, C. R. (2019). Kinematic and EMG analysis of horizontal bimanual climbing in humans. *J. Biomech.* **92**, 11-18. doi:10.1016/j.jbiomech.2019.05.023
Makhsous, M. (1999). Improvements, validation and adaptation of a shoulder model. *Doctoral Dissertation*, Chalmers University of Technology; Gothenburg, Sweden.
Mathewson, M. A., Kwan, A., Eng, C. M., Lieber, R. L. and Ward, S. R. (2014). Comparison of rotator cuff muscle architecture between humans and other selected vertebrate species. *J. Exp. Biol.* **217**, 261-273. doi:10.1242/jeb.083923
Matsen, F. A., Lippitt, S. B., Sidles, J. A. and Harryman, D. T. (1994). *Practical Evaluation and Management of the Shoulder*. Philadelphia, PA: W.B. Saunders.
McClure, P. W., Michener, L. A., Sennett, B. J. and Karduna, A. R. (2001). Direct three-dimensional measurement of scapular kinematics during dynamic movements in vivo. *J. Shoulder Elbow Surg.* **10**, 269-277. doi:10.1067/mse.2001.112954
Michilsens, F., Vereecke, E. E., D'Août, K. and Aerts, P. (2009). Functional anatomy of the gibbon forelimb: adaptations to a brachiating lifestyle. *J. Anat.* **215**, 335-354. doi:10.1111/j.1469-7580.2009.01109.x
Miller, D. K. (2006). *Measurement by the Physical Educator*, 5th edn. New York, New York, USA: McGraw-Hill Education.
Nelson, C. E., Rayan, G. M., Judd, D. I., Ding, K. and Stoner, J. A. (2017). Survey of hand and upper extremity injuries among rock climbers. *Hand* **12**, 389-394. doi:10.1177/1558944716679600
Nigg, B. M. and Herzog, W. (2007). *Biomechanics of the Musculo-Skeletal System*, 3rd edn. West Sussex, England: John Wiley & Sons Ltd.
Nussbaum, M. A. and Chaffin, D. B. (1996). Development and evaluation of a scalable and deformable geometric model of the human torso. *Clin. Biomech.* **11**, 25-34. doi:10.1016/0268-0033(95)00031-3
Oishi, M., Ogihara, N., Endo, H., Ichihara, N. and Asari, M. (2009). Dimensions of forelimb muscles in orangutans and chimpanzees. *J. Anat.* **215**, 373-382. doi:10.1111/j.1469-7580.2009.01125.x
O'Neill, M. C., Lee, L.-F., Larson, S. G., Demes, B., Stern, J. T., , Jr and Umberger, B. R. (2013). A Three-dimensional musculoskeletal model of the chimpanzee (Pan troglodytes) pelvis and hind limb. *J. Exp. Biol.* **216**, 3709-3723. doi:10.1242/jeb.079665
Oxnard, C. E. (1969). Evolution of the human shoulder: some possible pathways. *Am. J. Phys. Anthropol.* **30**, 319-331. doi:10.1002/ajpa.1330300302
Pontzer, H., Raichlen, D. A. and Sockol, M. D. (2009). The metabolic cost of walking in humans, chimpanzees, and early hominins. *J. Hum. Evol.* **56**, 43-54. doi:10.1016/j.jhevol.2008.09.001
Potau, J. M., Bardina, X. and Ciurana, N. (2007). Subacromial space in African great apes and subacromial impingement syndrome in humans. *Int. J. Primatol.* **28**, 865-880. doi:10.1007/s10764-007-9167-z
Potau, J. M., Bardina, X., Ciurana, N., Camprubí, D., Pastor, J. F., de Paz, F. and Barbosa, M. (2009). Quantitative analysis of the deltoid and rotator cuff muscles in humans and great apes. *Int. J. Primatol.* **30**, 697-708. doi:10.1007/s10764-009-9368-8
Pronk, G. M. (1991). The Shoulder Girdle, Analysed and Modelled Kinematically. *PhD Dissertation*. Department of mechanical engineering and marine technology, Delft University of Technology, Delft.
Punnett, L., Fine, L. J., Keyserling, W. M., Herrin, G. D. and Chaffin, D. B. (2000). Shoulder disorders and postural stress in automobile assembly work. *Scand. J. Work Environ. Health* **26**, 283-291. doi:10.5271/sjweh.544
Raichlen, D. A. (2006). Effects of limb mass distribution on mechanical power outputs during quadrupedalism. *J. Exp. Biol.* **209**, 633-644. doi:10.1242/jeb.02061
Rashedi, E., Kim, S., Nussbaum, M. A. and Agnew, M. J. (2014). Ergonomic evaluation of a wearable assistive device for overhead work. *Ergonomics* **57**, 1864-1874. doi:10.1080/00140139.2014.952682
Reghem, E., Chèze, L., Coppens, Y. and Pouydebat, E. (2013). Unconstrained 3D-kinematics of prehension in five primates: lemur, capuchin, gorilla, chimpanzee, human. *J. Hum. Evol.* **65**, 303-312. doi:10.1016/j.jhevol.2013.06.011
Regnault, S. and Pierce, S. E. (2018). Pectoral girdle and forelimb musculoskeletal function in the echidna (Tachyglossus aculeatus): insights into mammalian locomotor evolution. *R. Soc. Open Sci.* **5**, 181400. doi:10.1098/rsos.181400
Roach, N. T., Venkadesan, M., Rainbow, M. J. and Lieberman, D. E. (2013). Elastic energy storage in the shoulder and the evolution of high-speed throwing in *Homo*. *Nature* **498**, 483-486. doi:10.1038/nature12267
Roberts, D. (1974). Structure and function of the primate scapula. In *Primate Locomotion* (ed. F. A. Jenkins), pp. 171-200. New York: Academic Press.
Robling, A. G., Castillo, A. B. and Turner, C. H. (2006). Biomechanical and molecular regulation of bone remodeling. *Annu. Rev. Biomed. Eng.* **8**, 455-498. doi:10.1146/annurev.bioeng.8.061505.095721
Rooks, M. D. (1997). Rock climbing injuries. *Sports Med.* **23**, 261-270. doi:10.2165/00007256-199723040-00005
Ruff, C., Holt, B. and Trinkaus, E. (2006). Who's afraid of the big bad Wolff?: "Wolff's law" and bone functional adaptation. *Am. J. Phys. Anthropol.* **129**, 484-498. doi:10.1002/ajpa.20371
Schoonaert, K., D'Août, K. and Aerts, P. (2007). Morphometrics and inertial properties in the body segments of chimpanzees (*Pan* Troglodytes). *J. Anat.* **210**, 518-531. doi:10.1111/j.1469-7580.2007.00720.x
Schultz, A. H. (1968). The recent hominoid primates. In *Perspectives on Human Evolution. I* (ed. S. Washburn and P. C. Jay), pp. 122-195. New York, NY: International Thomson Publishing.
Scott, S. H. and Winter, D. A. (1991). A comparison of three muscle pennation assumptions and their effect on isometric and isotonic force. *J. Biomech.* **24**, 163-167. doi:10.1016/0021-9290(91)90361-P
Sonnabend, D. H. and Young, A. A. (2009). Comparative anatomy of the rotator cuff. *J. Bone Joint Surg.* **91-B**, 1632-1637. doi:10.1302/0301-620X.91B12.22370
Stern, J. T., , Jr and Larson, S. G. (2001). Telemetered electromyography of the supinators and pronators of the forearm in gibbons and chimpanzees: implications for the fundamental positional adaptation of hominoids. *Am. J. Phys. Anthropol.* **115**, 252-268. doi:10.1002/ajpa.1080
Stevens, N. J. and Carlson, K. J. (2008). Bridging gaps between experimental and naturalistic approaches in the study of primate behavior. *Int. J. Primatol.* **29**, 1395-1399. doi:10.1007/s10764-008-9310-5
Swindler, D. R. and Wood, C. D. (1973). *An Atlas of Primate Gross Anatomy: Baboon, Chimpanzee, and Man*. Seattle, Washington State: University of Washington.
Taylor, C. R., Shkolnik, A., Dmi'el, R., Baharav, D. and Borut, A. (1974). Running in cheetahs, gazelles, and goats: energy cost and limb configuration. *Am. J. Physiol.* **227**, 848-850. doi:10.1152/ajplegacy.1974.227.4.848
Teyhen, D. S., Miller, J. M., Middag, T. R. and Kane, E. J. (2008). Rotator cuff fatigue and glenohumeral kinematics in participants without shoulder dysfunction. *J. Athl. Train.* **43**, 352-358. doi:10.4085/1062-6050-43.4.352
Thompson, N. E., Ahmed, L., Celebi, T. B., Coopee, A. S., Koll, N., Rubinstein, D., Saunders, M. A. and Anemone, R. L. (2020). Digitization of the Nissen-Riesen chimpanzee radiological growth series. *Evol. Anthropol. Issues News Rev.* **29**, 173-179. doi:10.1002/evan.21836
Thorpe, S. K. S., Crompton, R. H., Günther, M. M., Kerr, R. F. and Alexander, R. M. (1999). Dimensions and moment arms of the hind- and forelimb muscles of common chimpanzees (Pan troglodytes). *Am. J. Phys. Anthropol.* **110**, 179-199. doi:10.1002/(SICI)1096-8644(199910)110:2<179::AID-AJPA5>3.0.CO;2-Z
Thorpe, S. K. S., Holder, R. L. and Crompton, R. H. (2007). Origin of human bipedalism as an adaptation for locomotion on flexible branches. *Science* **316**, 1328-1331. doi:10.1126/science.1140799
Thorpe, S. K. S., McClymont, J. M. and Crompton, R. H. (2014). The arboreal origins of human bipedalism. *Antiquity* **88**, 906-914. doi:10.1017/S0003598X00050778
Tsai, N.-T., McClure, P. W. and Karduna, A. R. (2003). Effects of muscle fatigue on 3-dimensional scapular kinematics. *Arch. Phys. Med. Rehabil.* **84**, 1000-1005. doi:10.1016/S0003-9993(03)00127-8
Turner, C. H. (2007). Skeletal adaptation to mechanical loading. *Clin. Rev. Bone Miner. Metab.* **5**, 181-194. doi:10.1007/s12018-008-9010-x
Usherwood, J. R., Larson, S. G. and Bertram, J. E. A. (2003). Mechanisms of force and power production in unsteady ricochetal brachiation. *Am. J. Phys. Anthropol.* **120**, 364-372. doi:10.1002/ajpa.10133
van Andel, C., van Hutten, K., Eversdijk, M., Veeger, D. J. and Harlaar, J. (2009). Recording scapular motion using an acromion marker cluster. *Gait Posture.* **29**, 123-128. doi:10.1016/j.gaitpost.2008.07.012
van der Helm, F. C. T. (1994). A finite element musculoskeletal model of the human shoulder mechanism. *J. Biomech.* **24**, 615-629.
Vaughan, C. L., Davis, B. L. and O'Connor, J. C. (1992). *Dynamics of Human Gait*. Champaign, IL: Human Kinetics.

Veeger, H. E. J. and van der Helm, F. C. T. (2007). Shoulder function: the perfect compromise between mobility and stability. *J. Biomech.* **40**, 2119-2129. doi:10.1016/j.jbiomech.2006.10.016

Voisin, J.-L. (2006). Clavicle, a neglected bone: morphology and relation to arm movements and shoulder architecture in primates. *Anat. Rec.* **288A**, 944-953. doi:10.1002/ar.a.20354

Voisin, J.-L., Ropars, M. and Thomazeau, H. (2014). The human acromion viewed from an evolutionary perspective. *Orthop. Traumatol. Surg. Res.* **100**, S355-S360. doi:10.1016/j.otsr.2014.09.011

Walker, A. (2009). The strength of great apes and the speed of humans. *Curr. Anthropol.* **50**, 229-234. doi:10.1086/592023

Ward, S. R., Hentzen, E. R., Smallwood, L. H., Eastlack, R. K., Burns, K. A., Fithian, D. C., Friden, J. and Lieber, R. L. (2006). Rotator cuff muscle architecture. *Clin. Orthop. Relat. Res.* **448**, 157-163. doi:10.1097/0000214443.87645.bb

Wood, B. A. and Richmond, B. G. (2000). Human evolution: taxonomy and paleobiology. *J. Anat.* **197**, 19-60. doi:10.1046/j.1469-7580.2000.19710019.x

Wood, J. E., Meek, S. G. and Jacobsen, S. C. (1989). Quantification of human shoulder anatomy for prosthetic arm control—I. Surface Modeling. *J. Biomech.* **22**, 273-292. doi:10.1016/0021-9290(89)90094-8

Wu, G., van der Helm, F. C. T., Veeger, H. E. J., Makhsous, M., Van Roy, P., Anglin, C., Nagels, J., Karduna, A. R., McQuade, K., Wang, X. et al. (2005). ISB recommendation on definitions of joint coordinate systems of various joints for the reporting of human joint motion. – Part II: shoulder, elbow, wrist and hand. *J. Biomech.* **38**, 981-992.

Xu, X., Lin, J.-H. McGorry, R. W. (2014). A regression-based 3-D shoulder rhythm. *J. Biomech.* **47**, 1206-1210. doi:10.1016/j.jbiomech.2014.01.043

Young, N. M. (2003). A reassessment of living hominoid postcranial variability: implications for ape evolution. *J. Hum. Evol.* **45**, 441-464. doi:10.1016/j.jhevol.2003.09.001

Young, N. M. (2005). Estimating hominoid phylogeny from morphological data: character choice, phylogenetic signal and postcranial data. In *Interpreting the Past: Essays on Human, Primate and Mammal Evolution in Honor of David Pilbeam* (ed. D. E. Lieberman, R. J. Smith and J. Kelley), pp. 19-31. Boston, MA: Brill Academic Publishers, Inc.

Young, N. M. (2008). A comparison of the ontogeny of shape variation in the anthropoid scapula: functional and phylogenetic signal. *Am. J. Phys. Anthropol.* **136**, 247-264. doi:10.1002/ajpa.20799

Young, N. M., Capellini, T. D., Roach, N. T. and Alemseged, Z. (2015). Fossil hominin shoulders support an African ape-like last common ancestor of humans and chimpanzees. *Proc. Natl. Acad. Sci. USA* **112**, 11829-11834. doi:10.1073/pnas.1511220112

Zihlman, A. L. (1992). Locomotion as a life history character: the contribution of anatomy. *J. Hum. Evol.* **22**, 315-325. doi:10.1016/0047-2484(92)90062-E